

# Assessing small area estimates via bootstrap-weighted k-Nearest-Neighbor artificial populations

Grayson W. White, Jerzy A. Wieczorek, Zachariah W. Cody, Emily X. Tan, Jacqueline O. Chistolini, Kelly S. McConville, Tracey S. Frescino, and Gretchen G. Moisen<sup>1</sup>

## Abstract

Comparing and evaluating small area estimation (SAE) models for a given application is inherently difficult. Typically, many areas lack enough data to check unit-level modeling assumptions or to assess unit-level predictions empirically; and no ground truth is available for checking area-level estimates. Design-based simulation from artificial populations can help with each of these issues, but only if the artificial populations realistically represent the application at hand and are not built using assumptions that inherently favor one SAE model over another. In this paper, we borrow ideas from random hot deck, approximate Bayesian bootstrap (ABB), and  $k$  Nearest Neighbor (kNN) imputation methods to propose a kNN-based approximation to ABB (KBAABB), for generating an artificial population when rich unit-level auxiliary data is available. We introduce diagnostic checks on the process of building the artificial population, and we demonstrate how to use such an artificial population for design-based simulation studies to compare and evaluate SAE models, using real data from the Forest Inventory and Analysis (FIA) program of the US Forest Service.

## 1 Introduction

The USDA 2014 and 2018 Farm Bills (*Agricultural Act of 2014* 2014; *Agriculture Improvement Act of 2018* 2018) direct the Forest Inventory and Analysis (FIA) Program to: “implement procedures to improve the statistical precision of estimates at the sub-State level” and “find efficiencies in the operations of the Forest Inventory and Analysis Program under section 3(e)

1. Grayson W. White, Dept. of Forestry and Dept. of Statistics & Probability, Michigan State University, East Lansing, MI, USA; Jerzy A. Wieczorek (ORCID 0000-0002-2859-6534), Zachariah W. Cody, Emily X. Tan, and Jacqueline O. Chistolini (ORCID 0000-0002-3594-3573), Department of Statistics, Colby College, Waterville, ME, USA; Kelly S. McConville, Department of Statistics, Harvard University, Cambridge, MA, USA; Tracey S. Frescino and Gretchen G. Moisen, Forest Inventory and Analysis, Rocky Mountain Research Station, USDA Forest Service, Ogden, UT, USA.

of the Forest and Rangeland Renewable Resources Research Act of 1978 (16 U.S.C. 1642(e)) through the improved use and integration of advanced remote sensing technologies to provide estimates for State- and national-level inventories, where appropriate.” The FIA program (<https://www.fs.usda.gov/research/programs/fia>) provides data and tools for delivering standardized estimates at state levels over 5-10 year periods, but there is currently no standardized methodology to generate estimates at these sub-State levels or shorter time intervals. The need for more precise information of ecological characteristics and integrity at sub-State levels is essential for field specialists and managers to make tactical assessments for local and broad-scale monitoring and planning. In response to the Farm Bill initiatives, FIA is working towards a strategic plan to define FIA user needs, evaluate small area estimation (SAE) methodology, and deliver statistically sound, standardized estimates to users at the sub-State level.

Estimation of the biomass of live trees is specifically referenced in the Farm Bill initiatives but additional examples of the survey variables FIA collects include number of trees per acre, basal area of trees per acre, above ground carbon of trees per acre, etc., while the auxiliary variables available for use in SAE models come from satellite data, climate records, elevation models, etc.

SAE methods are designed to address the limitations of small sample sizes in unplanned domains, but understanding the best SAE method to use for each particular FIA application is still an open question. More broadly, empirically comparing and evaluating SAE models is an inherently challenging problem (Brown et al. 2001; Rao and Molina 2015; Dorfman 2018; Tzavidis et al. 2018). While there exist many useful model-comparison tools for unit-level predictive models (for instance, cross-validation, or information criteria such as AIC and BIC), these tools are often of limited use for SAEs. Sometimes we do not have unit-level data, only area-level. Even when we do have unit-level data, what we really want to assess are the area-level estimates, not the unit-level predictions themselves. In both cases, area-level direct estimates from the sample itself are not precise enough to be treated as ground truth for model comparisons; we cannot rely on checking whether the model-based estimate is close to the direct estimate for each area.

Let  $P = \{(X_i, Y_i)\}$ ,  $i \in 1, \dots, N$  denote the complete finite population  $P$  of size  $N$ , where

each  $X_i$  is a  $p$ -dimensional vector of auxiliary data and  $Y_i$  is the response variable whose means we wish to estimate in each small area. In practice, we do not observe all of  $P$  but a sample  $S = \{(X_i, Y_i)\}$ ,  $i \in s$  where  $s \subset \{1, \dots, N\}$  is drawn using some known sampling design  $D$ . Typically  $D$  is chosen so that the sample means of  $Y$  in  $S$  have adequate precision for estimating the population means of  $Y$  in  $P$  as a whole. But if we also wish to estimate the population means of  $Y$  for domains or small areas—subpopulations of  $P$ —and some or all of these domains do not have an adequate sample size to estimate these domain means precisely, we call this a SAE problem.

Dorfman (2018) lists a “Variety of Inadequate Methods of Evaluation” for SAE, including “(7) large scale *simulation studies* from administrative, census or large samples—these can give useful insights but satisfactory extrapolation to the case at hand has to be assumed[. . .]” From the design-based perspective, such simulation studies are most straightforward to justify if they consist of repeated sampling using  $D$  from a real and relevant population, either  $P$  itself or complete administrative or census records of recent vintage (Lehtonen and Veijanen 2009; Tzavidis et al. 2018), but a complete real population is rarely available. Alternately, simulation studies can consist of repeated sampling using  $D$  from an *artificial* population  $\hat{P}$  (Alfons et al. 2011; Wieczorek, Nugent, and Hawala 2012; Wieczorek and Franco 2013; Templ et al. 2017), but this requires extra care to justify why the artificial population resembles the real one in the relevant sense: How can we trust that model assessment across samples  $S_1^*, S_2^*, \dots$  drawn using  $D$  from the artificial population  $\hat{P}$  should be informative about model performance on our *real* sample  $S$  from the *real* population  $P$ ?

In the present paper, we describe a novel approach to generating one or more artificial populations: a “kNN-based approximation to the approximate Bayesian bootstrap” (KBAABB). We justify why KBAABB can allow for “satisfactory extrapolation” from simulation studies. We illustrate how to use our artificial population for model evaluation and comparison, following approaches and metrics similar to those in Dorfman (2018) and Wieczorek, Nugent, and Hawala (2012).

Briefly, in our setting we have complete auxiliary data  $X$  for the entire population of inter-

est  $P$ , but a much smaller survey sample  $S$  of the joint auxiliary and response variables  $(X, Y)$ . To generate a complete artificial population  $\hat{P}$ , we wish to impute response values from the observed survey data (donor dataset) to every row of the full-population auxiliary data (recipient dataset). We begin with the approximate Bayesian bootstrap (ABB), a multiple imputation tool that approximates the process of drawing from a posterior distribution for the missing data given the observed data (Rubin and Schenker 1986). We use bootstrap-weighted sampling with kNN to implement KBAABB, a computationally-cheaper approximation of ABB, defined precisely in Section 2.1. The resulting artificial population can be interpreted as one draw from a posterior distribution for the population’s response values.

A single run of KBAABB produces one artificial population, from which we repeatedly draw smaller samples using the FIA’s real sampling design. This allows us to carry out design-based simulations in a finite-population framework. In addition, repeated runs of KBAABB could easily produce multiple artificial populations, allowing for simulations under a superpopulation framework (Isaki and Fuller 1982) and/or Bayesian posterior inference, although we do not do so in this paper.

Empirically, we show that the output of KBAABB on our FIA dataset is comparable to or better than artificial populations built via other imputation methods commonly used in practice: single nearest neighbor (NN) imputation, and unweighted kNN imputation where each donor is selected uniformly at random from a donor pool of the recipient’s  $k$  closest neighbors (Andridge and Thompson 2023). KBAABB avoids the worst-case risks of single NN and the *ad hoc* nature of unweighted kNN.

Our artificial population  $\hat{P}$  is designed to have the correct marginal distribution of  $X$  and a reasonable estimate of the conditional distributions of each  $Y|X$ , and our samples from the artificial population accurately represent the real sampling design. However, we do not claim that the area-level means from  $\hat{P}$  are correct for  $P$ . Rather, we will use  $\hat{P}$  to seek SAE methods that tend to produce good estimates—close to the “artificial truth” of  $\hat{P}$ ’s area-level means—when fitted to samples drawn using  $D$  from  $\hat{P}$ .

## 1.1 Related work

Other work on realistic artificial populations for design-based simulations typically relies only on the survey dataset itself, or on the survey data combined with population summaries of the auxiliary variables rather than a complete unit-level dataset. Alfons et al. (2011) generate fully-synthetic artificial populations through a combination of weighted sampling from the real survey data and model-based simulation from parametric models fit to the real survey data. Wieczorek and Franco (2013) treat a large sample as the full artificial population and mimic the real sampling design to take smaller subsamples from it for the purpose of evaluating SAE models. Beyond the survey dataset alone, if full-population marginal totals or cross-tabulations for the auxiliary data are also available, e.g. tables from a recent census, Templ et al. (2017) summarize approaches to generating an artificial population by resampling entire rows from the survey data until the artificial population meets these marginal or cross-tabulated constraints. However, none of the above approaches make use of the rich unit-level auxiliary data that is available in our FIA setting.

Another approach is to make up a parametric model (or fit one to the sample); make a prediction  $\hat{Y}(X_i)$  for each row of the  $X$ s; and add random noise to each prediction to generate the artificial population's  $Y$ s (Morris, White, and Royston 2014). However, under this approach, the artificial population would inherently favor SAE models of the same parametric form. If some of the models we wish to evaluate are correct for the artificial population but mis-specified for the real population, then simulation studies on the artificial population would be overly optimistic for these models. Instead, KBAABB's nonparametric kNN-based matching ensures that the artificial population will not have a bias towards being fit well by any of the common parametric SAE models, yet our imputed  $Y$  values will still have realistic conditional distributions for  $Y|X$ . Of course, if we also planned to evaluate the use of kNN-based models for SAEs, then we would want to choose a different non-kNN model to generate our artificial population (Baffetta et al. 2009).

Andridge and Little (2010) review the literature on hot deck and kNN imputation methods. They point out that although kNN makes fewer assumptions than parametric models, it does

rely on implicit assumptions defined by our choices of what variables to match on and what distance metric to use. Also, kNN methods only make sense if there are at least a few donors “near” every recipient, in the  $X$  space. Finally, a downside to kNN-based approaches like KBAABB is that we can never impute plausible  $Y$  values that exist in the real population but were not observed in the sample survey data. We did not deem this to be a major concern in our FIA example, because we had observed several thousand distinct response values for each  $Y$  variable in our survey dataset and they covered most of the range of plausible population values for each  $Y$  variable.

While our primary goal is to generate artificial populations for model evaluation, KBAABB could also be useful in other settings where we need to generate large, realistic, complete datasets: multiple imputation for missing data; statistical matching for data fusion; and synthetic micro-data for disclosure avoidance or microsimulation.

## 1.2 Data

Our simulation study area is the M333 Northern Rocky Mountain Forest-Steppe-Coniferous Forest-Alpine Meadow Province from the US Forest Service’s national hierarchical framework of ecological units (Cleland et al. 2007; ECOMAP 1993). EcoMap provinces are delineated by climatic zones and broad vegetation types with further delineations into sections and subsections, representing different geomorphic and topographic features (ECOMAP 1993). The M333 province stretches across western Montana, through Northern Idaho, to eastern Washington and is about 98,700 km<sup>2</sup> in size. The province encompasses four mountainous sections, with an average of six subsections each, twenty-three in total. These are our 23 domains (Figure 1).

The FIA program surveys a sample of field plot locations across the US based on a hexagonal grid. Each plot samples approximately 2.5 acres (1.0 ha) of land and represents approximately 6000 acres (2428 ha) of land within each hexagon (McRoberts et al. 2005; Bechtold and Patterson 2005). Attributes are measured and observed at each survey plot location and stored in FIA’s national database (Burrill et al. 2021). We extracted data from FIA’s database (last updated 2021 July 8) on 20 July 2021. There are 3946 survey plots across the 23 domains, with

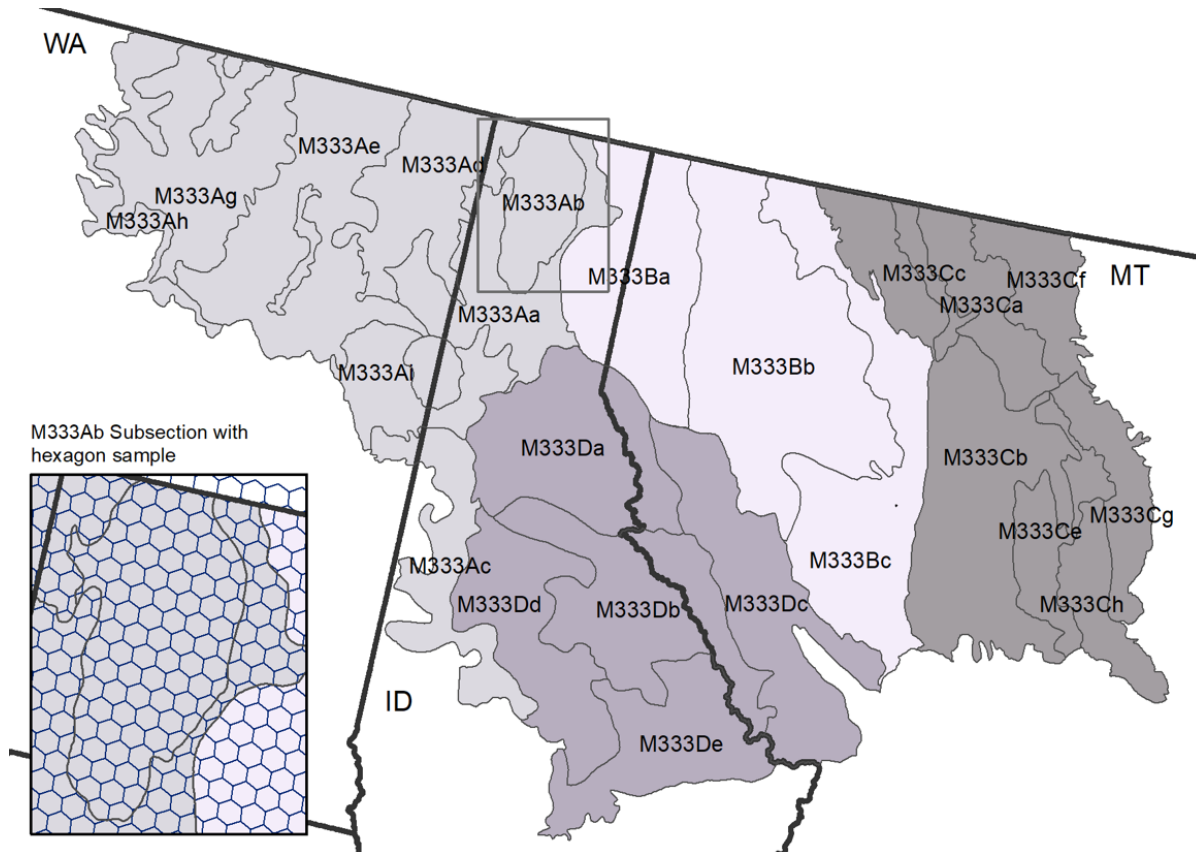


Figure 1: Simulation study area.

Table 1: Y-variables or survey variables recorded by field crews at each surveyed plot.

Variable	Units	Description
BA	square feet	Basal area of live trees
VOLCFNET	cubic feet	Net cubic-foot volume in sawlog portion of a live sawtimber tree
VOLBFNET	board feet	Net board-foot volume in sawlog portion of a live sawtimber tree
COUNT	number	Number of live trees per acre unadjusted
DRYBIO	tons	Aboveground biomass of live trees (Heath et al. 2009)
CARBON	tons	Aboveground carbon of live trees (Heath et al. 2009)

Table 2: X-variables or auxiliary variables.

Variable	Units	Description
tcc	%	National Land Cover Dataset (NLCD) Analytical Tree Canopy Cover (Yang et al. 2018)
elev	meters	LANDFIRE 2010 DEM - elevation (U.S. Geological Survey 2019)
eastness	(-100 to 100)	Transformed aspect degrees to eastness (U.S. Geological Survey 2019)
northness	(-100 to 100)	Transformed aspect degrees to northness (U.S. Geological Survey 2019)
tri	index	Terrain Ruggedness Index (U.S. Geological Survey 2019)
tpi	index	Topographic Position Index (U.S. Geological Survey 2019)
ppt	mm $\times$ 100	PRISM mean annual precipitation - 30yr normals (1991-2020) (Daly et al. 2002)
tmin01	$^{\circ}\text{C}\times 100$	PRISM mean minimum temperature (Jan) - 30yr normals (Daly et al. 2002)
wc2c1	class	Eur. Space Agency (ESA) 2020 WorldCover global land cover (Zanaga et al. 2021)
tnt	class	LANDFIRE 2014 tree/non-tree lifeform mask (Rollins 2009; Picotte et al. 2019)

98% of the plots measured between 2010 and 2019. From these plots, we compile our Y-variables and associated X-variables.

Our Y-variables were all aggregated to the plot level. These variables were: basal area (BA), net cubic-foot volume (VOLCFNET), net board-foot volume (VOLBFNET), number of trees (COUNT), aboveground dry biomass (DRYBIO), and aboveground carbon (CARBON). See Table 1 for further details.

We also have auxiliary X-variables from satellites, climate records, and digital elevation models that were thought to relate to and discriminate our Y variables (Table 2). The auxiliary information includes surface reflectance images, including spectral indices and classified imagery to get a picture of vegetation on the ground (Schwager and Berg 2021) and both broad-scale and localized climatic characteristics to understand ecological tolerances. All auxiliary data were re-sampled from their original resolution to 90x90m pixels. For each plot, we have the auxiliary data corresponding to that plot’s location. Although more auxiliary variables could have been used, our kNN matching steps only used the categorical variable `wc2c1` for stratification and the quantitative variables in Table 2 for matching. Some of our analyses in Section C used `tnt` for post-stratification.



As a basis for the artificial population, besides the survey sample we also have complete auxiliary-only data for the full population: 11,752,067 pixels in the 4286 hexagons that fall within or overlap with EcoProvince M333. The largest hexagon had 2979 pixels, and the median was 2964, although several hexagons along the edge of the province had just a few pixels in the target population. For each of these auxiliary-only pixels, we had the same  $X$  variables as for the 3946 pixels corresponding to the real survey plots.

We use an analysis function in the `FIESTAanalysis` R package (which is an extension of the `FIESTA` R package), `anGetPixelDat()`, to generate pixel-level data tables for each subsection (Frescino and White 2022; Frescino et al. 2023). The function creates a table of a combination of longitude and latitude extracted from each 90x90m pixel across each subsection, including a unique identifier of each pixel. This table is then used to extract values of our auxiliary information to create a set of data for our simulation models.

## 2 Population Generation and Design-Based Sampling

### 2.1 Population Generation with KBAABB

With rich auxiliary data for the entire population, we can treat the unobserved response values in our population as missing data that needs to be imputed. Several popular approaches to imputation of missing data are based on nearest neighbors (NN).

In the single NN approach, each recipient row is matched to the “nearest” donor row—the donor row whose auxiliary variables are most similar to the recipient’s by some distance metric—and that donor’s response variables are imputed to that recipient. However, this approach risks overusing the same donor for all recipients with similar  $X$  values, which could result in unrealistically low variability in the imputed  $Y$  values (Andridge and Thompson 2023). For the same reason, imputing the means or medians of larger donor pools (Crookston and Finley 2008) is also unsuitable for our purposes.

An alternative is to use a recipient’s  $k$  nearest neighbors (kNN) as the donor pool, for a  $k$  such as 5, 10, or 20 (Morris, White, and Royston 2014), and then to choose one case in this

donor pool *uniformly at random* to be imputed to the recipient (Andridge, Bechtel, and Thompson 2021). This avoids single NN’s problem of always imputing the same donor—but it can also lead to bias in the imputed conditional distributions of  $Y|X$ , since a larger donor pool may include  $Y$  values that are not realistic for the recipient’s  $X$  values. It also requires careful choice of  $k$ . (In the extreme case,  $k = n$  would replace every imputed conditional distribution of  $Y|X$  with an imputed marginal distribution of  $Y$ .)

Our proposed method, KBAABB, works like kNN imputation but with uniform random sampling of donors replaced by weighted sampling, with the weights based on bootstrap selection probabilities. The  $j^{\text{th}}$  NN is selected with probability  $p_b \times (1 - p_b)^{j-1}$ , where  $p_b = 1 - e^{-1} \approx 0.632$  is the asymptotic probability of an observation being selected into a bootstrap sample (Andridge and Thompson 2023). See inner loop of Algorithm 1. Furthermore, to reduce bias and variance, KBAABB can be applied independently within strata; and to avoid sensitivity to units of measurement, the auxiliary variables can be centered and scaled before calculating Euclidean distances to find the  $k$  NNs for each recipient. See outer loop of Algorithm 1 and Section 2.3.

If there are several response  $Y$  variables to be imputed for each recipient, KBAABB imputes all of them from the same donor to their recipient. If instead we were to impute each response variable independently, our artificial population would not accurately reflect the associations among these variables (Andridge and Little 2010; Nur et al. 2005).

In principle, by selecting nearer neighbors with higher probability, KBAABB should avoid the pitfalls of single NN (too little variability in  $Y$ ) and kNN (bias due to large  $k$ ), while also removing the need to choose tuning parameter  $k$ . Empirically, in the Supplemental data, Appendix A, we report a sensitivity analysis regarding the probabilities of selection and the choice of  $k$ , comparing KBAABB to unweighted kNN approaches on our FIA dataset. For each response variable  $Y$ , we found the same results: As kNN’s  $k$  grows, the distribution of  $Y$  in each domain becomes more similar across domains, and unweighted  $k = 20$  or larger makes the domains too similar to each other. Furthermore, when looking at spatial maps of the imputed  $Y$  values, the spatial patterns look realistically smooth for single NN and for KBAABB, but begin to look unrealistically noisy for unweighted  $k = 5$  or larger.

**Algorithm 1** KBAABB, with stratification and standardization

---

```

for  $j = 1$  to 9 do ▷ Define the selection probabilities
   $\mathbb{P}(j\text{th ranked NN selected}) \leftarrow \exp(-j + 1) \times (1 - \exp(-1))$ 
end for
 $\mathbb{P}(10\text{th ranked NN selected}) \leftarrow 1 - \sum_{j=1}^9 \mathbb{P}(j\text{th ranked NN selected})$ 

for  $\text{stratum} \in \{\text{strata}\}$  do ▷ Process each stratum separately
   $\text{recipients} \leftarrow \{\text{all population units} \in \text{stratum}\}$ 
   $\text{donors} \leftarrow \{\text{all sample units} \in \text{stratum}\}$ 
  Center/scale auxiliary data in  $\text{recipients}$  and  $\text{donors}$ , using  $\text{recipients}$  means and SDs

  for  $\text{unit} \in \text{recipients}$  do ▷ kNN matching and ABB imputation
     $\text{NNs} \leftarrow 10$  nearest neighbors in auxiliary data space to  $\text{unit}$  from  $\text{donors}$ 
    Rank  $\text{NNs}$  by distance to  $\text{unit}$  in auxiliary data space from  $j = 1$  to 10
    Randomly sample one element of  $\text{NNs}$  based on  $\mathbb{P}(j\text{th ranked NN selected})$ 
    Impute all response values from selected element of  $\text{NNs}$  to  $\text{unit}$ 
  end for
end for

```

---

## 2.2 Heuristic Rationale for Bootstrap Weighting

KBAABB’s use of bootstrap weights is heuristically inspired by the approximate Bayesian bootstrap (ABB) (Rubin and Schenker 1986). ABB is popular for multiple imputation because it is provably “valid,” loosely meaning that it allows asymptotically unbiased design-based inferences under both the sampling and the nonresponse mechanisms; for details, see Chapter 4 of Rubin (2004). In Bayesian inference, one run of ABB can also be treated as one draw from a posterior distribution for the population’s response values, given the survey sample and the full-population auxiliary values and using a nonparametric model for the likelihood. Neither “validity” nor Bayesian inference are central to our goal of creating an artificial population, but ABB inspired us to try bootstrap weighting, and empirically we have found it to be a success in our case study; see Supplemental data, Appendix A.

Briefly, our bootstrap weights arise from mimicking true ABB, where we would first draw a bootstrap sample from the complete-data cases, then draw with replacement from this bootstrap sample to impute the missing cases. In order to reduce both bias and variance, typically ABB imputes from a smaller donor pool based on some auxiliary information. If we use a single NN from the bootstrap sample to define the donor pool for each recipient, around  $p_b$  of recipients

will have their NN from the original sample selected as their donor (Andridge and Thompson 2023). However, NN with true ABB is still computationally expensive for our task of generating an artificial population, as we would need to take a new bootstrap sample of the complete-case survey data for every recipient, then redo the NN search for that recipient. KBAABB is a computational shortcut: Use the original sample (not a resample) to find a donor pool of  $k$  NNs for each recipient row separately, then use bootstrap-weighted sampling to choose one donor for that recipient. Under true ABB with NN, each recipient has approximately a  $(1 - p_b)^{j-1} \times p_b$  probability that the first  $j - 1$  NNs would not be in the bootstrap sample but the  $j^{\text{th}}$  would be. (This probability becomes negligible quickly, so in practice we only find the  $k = 10$  NNs and select the  $10^{\text{th}}$  NN with probability  $1 - \sum_{j=1}^9 (1 - p_b)^{j-1} \times p_b \approx 0.000124$ .) Thus, KBAABB’s bootstrap weights approximate the process of running NN with true ABB once per recipient.

### 2.3 Choices to be made during KBAABB Implementation

To implement KBAABB, as with any other kNN-based method we must decide how to define “nearest” for the kNN search: Which variables, transformations, and distance metric should be used to rank the donor pool for each recipient?

First, if the population consists of strata or post-strata for which units tend to be homogeneous within strata but quite different across strata, KBAABB will have less bias and less unnecessary variability if kNN matching is carried out separately in each stratum.

Next, kNN is known to suffer from the curse of dimensionality: if we use Euclidean distance in a high-dimensional space, the several nearest neighbors might all be very far away (James et al. 2021). When there are many auxiliary variables available for matching, NN imputation can be asymptotically biased and some analysts prefer to summarize the auxiliary variables into a univariate matching variable (Morris, White, and Royston 2014; Yang and Kim 2019). However, to keep the matching process as model-free as possible, others may prefer to simply reduce the matching space to a subset of the variables, using subject matter expertise. Such parsimony can also reduce unnecessary variance in the matching process D’Orazio 2015.

Furthermore, if matching variables are heavily skewed, it may be worthwhile to transform

them to be more symmetric. Otherwise, donors with distant outlier values might never be one of the nearest neighbors for any recipient. Chen and Shao (2000) show that for imputation purposes, NN imputation can be biased when the matching variables are not symmetric.

We may also center and scale each of the matching variables to have mean 0 and standard deviation 1 (within each stratum separately) on the full-population auxiliary dataset. The same centering and scaling constants (by class and variable) should be applied to the smaller survey sample dataset. This removes the effect of different variables having different units and scales, ensuring that each variable is given equivalent weight in the kNN matching process (James et al. 2021).

Finally, a distance metric must be chosen and computed between each recipient and each donor using the selected and transformed variables. If the selected variables are not strongly correlated with each other and they have been centered and scaled transformations, a simple Euclidean distance might suffice. Alternatives such as e.g. Mahalanobis distance could account for covariances between variables (Crookston and Finley 2008).

## 2.4 Empirical Diagnostics for KBAABB

We describe several ways to check whether the artificial population generated with KBAABB look reasonable, or whether choices made as described in Section 2.3 need to be re-evaluated. For examples illustrating each of these checks, see Supplemental data, Appendix B.2.

First, we can compare the statistical distributions of the imputed  $Y$  variables to the original survey. We may judge each  $Y$  marginally by looking at histograms or empirical CDFs for the  $Y$  values from KBAABB vs. from the original survey. We can also look at their associations with each other, or with other variables, by looking at pairwise scatterplots, again comparing the imputed vs. original data. Conditionally by domain, we can calculate summary statistics such as SDs in each domain and again compare them for the imputed vs. original  $Y$  values.

In a setting where there are spatial coordinates for each observation, we can also compare the spatial smoothness of the imputed  $Y$  variables to that of similar  $X$  variables. This can be as simple as using color to represent the imputed  $Y$  values for each pixel on a geographic map

and judging whether it looks much noisier or smoother than a corresponding heatmap of  $X$ . If heatmaps look substantially different for the imputed  $Y$ s than for the  $X$ s, the kNN matching variables or distance metric might not be capturing meaningful spatial trends in the data. Another approach is to compare measures of spatial autocorrelation such as Moran’s I (Moran 1950).

Additionally, we can check whether donation patterns look reasonable. First, how often was each donor selected to be in some recipient’s donor pool, and how often was it actually chosen to be a donor? If some donors are never used, the kNN matching may be overusing others. Next, in a SAE situation where the population is partitioned into domains and we expect observations within a domain to be more similar within than across domains, we can check for imbalances in how often each recipient’s domain matched the donor’s domain. For each row in the artificial population, cross-tabulate the domain of each recipient vs. its donor. We hope to see moderate but not complete association between the donor and recipient domains. If both are always from the same domain, the artificial population may be too similar to a copy of the survey sample. On the other hand, if recipients come from every donor domain uniformly, recipients may be getting donors which do not actually resemble them.

## 2.5 Sampling for Design-Based Simulations

For each replication (“rep”) of a survey sample from the KBAABB-generated artificial population, we take a sample using the same sampling design  $D$  that was used to draw the real sample. This lets us carry out design-based simulations which respect the sampling design of the actual survey data. When we fit a given SAE model form to each rep, and then summarize the model’s empirical properties across reps, these properties are reasonable stand-ins for what we could expect to see under repeated sampling from the real sampling design.

Optionally, we could also add a simulated non-response stage after the sampling stage, to mimic any non-response behavior seen in the real survey.

### 3 Case Study: Using KBAABB to Evaluate SAEs

The artificial population generated with KBAABB allows for an extensive evaluation of SAE methods and strategies that may be implemented by researchers and others interested in the performance of small area estimators under a variety of conditions. In order to evaluate such small area estimators, we created 2500 samples from the artificial population, where we sampled one pixel per hexagon for each hexagon that overlaps M333, as described in Section B.3. The small area estimators are assessed based on their estimates and MSE estimates of average basal area (BA) per unit area within each subsection in M333. We have chosen to assess four commonly applied estimators in the SAE literature to give a sense of what can be done with KBAABB through a basic yet illustrative example. In particular, we implemented the Horvitz-Thompson (Horvitz and Thompson 1952), modified generalized regression (GREG) (Woodruff 1966; Wojcik et al. 2022), area-level empirical best linear unbiased prediction (EBLUP) Fay-Herriot (Fay and Herriot 1979), and unit-level EBLUP Battese-Harter-Fuller (Battese, Harter, and Fuller 1988) estimators. Model-based and -assisted estimators used auxiliary variables `tcc`, `tri`, and `elev`, which are defined in Table 2.

We considered four evaluation metrics in this case study: relative bias, MSE, MSE ratio, and 95% confidence interval coverage. The relative bias is defined as, for a particular estimator ( $i$ ) and subsection ( $j$ ),

$$\frac{\mathbb{E}[\hat{\mu}_{ij}] - \mu_j}{\mu_j}$$

where  $\mu_j$  is the true mean biomass in subsection  $j$  as generated by KBAABB and  $\mathbb{E}[\hat{\mu}_{ij}]$  is defined as follows,

$$\mathbb{E}[\hat{\mu}_{ij}] = \frac{1}{K} \sum_{k=1}^K \hat{\mu}_{ijk}, \quad (1)$$

i.e., the empirical expected value for estimator  $i$  of mean biomass in subsection  $j$  across all reps.

The MSE for a given estimator and subsection is given by

$$\text{MSE}_{ij} = \frac{1}{K} \sum_{k=1}^K (\hat{\mu}_{ijk} - \mu_j)^2.$$

The MSE ratio is defined as the ratio of the empirical expected value of the MSE estimator and the empirical MSE for a particular estimator and area of interest,

$$\frac{\mathbb{E}[\widehat{\text{MSE}}_{ij}]}{\text{MSE}_{ij}}$$

where  $\mathbb{E}[\widehat{\text{MSE}}_{ij}]$  is the empirical expected value of the MSE estimator for estimator  $i$  in subsection  $j$  across all reps, defined analogously to Equation 1. The 95% confidence interval coverage is defined as, for a particular estimator and subsection, the proportion of samples across all reps where a given estimator's 95% confidence interval contains  $\mu_{ij}$ .

In order to assess the metrics described above, we turn to Figure 2. Each subfigure displays a metric for each subsection and estimator combination; in particular subfigure A displays the relative bias, subfigure B displays the MSE, subfigure C displays the MSE ratio, and subfigure D displays the confidence interval coverage. For the two design-based estimators, the relative bias remains low, as we would expect. However, for the model-based estimators we see a larger spread of values for relative bias. On median, the area- and unit-level EBLUP estimators exhibit negative and positive relative bias, respectively. Further, the distribution of the area-level EBLUP's bias is primarily negative, with its interquartile range entirely following below the 0 on the y-axis. While examining the empirical relative bias can be informative, it can also be useful to look at the distribution of estimates produced over each simulation rep in order to get a fuller sense of the estimator's performance across samples. This is shown in Figure 3. From Figure 2 alone we might be concerned with some of the biases that the Horvitz-Thompson estimator is exhibiting, but upon examination in Figure 3 we can see how variable the estimator is, and that it does not appear to be producing concerning bias in any subsection. Contrastingly, the model-based estimators display some more concerning characteristics: in subsections such as M333Ah (Okanogan Semi-Arid Foothills) and M333Cc (Mission-Swan Valley-Flathead



River), we see the model-based estimators producing precise estimates that are consistently over- or under-estimating the parameter of interest, leading to bias in the estimator. This bias may be attributed to a variety of causes, but upon ecological inspection of the subsections, we see that, compared to the rest of the M333 province, these are lower elevation regions which likely exhibit very different qualities than the otherwise mountainous majority of M333, making it difficult for the model's random effect to pool accurately. The modified GREG estimator is both moderately precise and exhibits less concerning distributions than the model-based approaches, although the modified GREG does still have trouble capturing the true mean in M333Ah.

Returning to Figure 2, we see in subfigure B the MSE of model-based and -assisted estimators are competitive in this case study, with the two model-based approaches exhibiting the lowest MSE on median, but the modified GREG estimator displaying similar values. Subfigure C displays the MSE ratio, i.e. how well an estimator's MSE is estimated, and we see here the Horvitz-Thompson and modified GREG estimators with values right around 1, and the model-based estimators show an overestimation of MSE, on median. Further, in subfigure D we see the 95% confidence interval coverage looks very sensible for the Horvitz-Thompson and modified GREG estimators, and slightly more instances of over- or under-coverage for the model-based estimators. This makes sense in light of subfigure C where we see an over-estimation of the uncertainty in these estimators.

In light of Figure 2, subfigure C, we wanted to understand if the poor MSE estimation of some estimators can be attributed to any systematic properties in the areas of interest, and to assess this we turn to Figure 4, which displays the MSE ratio by proportion of zero-valued pixels in the population for the response variable, with points sized by MSE. The Horvitz-Thompson, modified GREG, and area-level EBLUP estimator do not exhibit a relationship between the displayed variables; however, we see that the area-level EBLUP does over-estimate the MSE for subsections with small MSEs, and under-estimates MSE for subsections with large MSEs. This is somewhat expected with the pooling that occurs when fitting a mixed model. We also see this trend for the unit-level EBLUP estimator. Strikingly though, the unit-level EBLUP estimator's MSE ratio has a strong positive linear relationship with the proportion of zero-valued

pixels in the population for the response variable. We see that when the proportion of zero-valued pixels is greater than approximately 0.1, the MSEs tend to be smaller but are also over-estimated. This is likely due to model-misspecification that can occur at the unit-level due to zero-inflation in the data. The forest inventory data used here is positive and continuous sans zeros, and we expect as the proportion of zeros in a subsection increases, that the model will be increasingly misspecified. Zero-inflated estimators have been proposed to deal with the model-misspecification discussed here (Finley, Banerjee, and MacFarlane 2011; White et al. 2024), but this systematic issue in estimating the MSE of small area estimates is not discussed. In order to obtain the precision of a unit-level, model-based approach without the perils of the unit-level EBLUP shown here, it may be worthwhile to consider the approaches taken by Finley, Banerjee, and MacFarlane (2011) or White et al. (2024).

From this case study, we are able to obtain much information about the estimators considered. First of all, the Horvitz-Thompson estimator appears to be performing as we expect, which is a good check that our simulation is producing sensible results. Next, the modified GREG and area-level EBLUP both appear to be decent estimators for these data and areas of interest. Both estimators produce sensible estimates; however, in some outlying subsections we do see estimator bias appear. Finally, the unit-level EBLUP displays concerning results regarding poor and systematic over-estimation of the MSE. While the unit-level EBLUP was the most precise estimator in terms of MSE (on median, Figure 2), its MSE estimation was unreliable. Given the choice between the four estimators, the modified GREG has the best balance of low bias, low MSEs, accurate MSE estimation, and correct confidence interval coverage.

## 4 Discussion

Our kNN-based approximation to ABB is suitable when we have rich and complete auxiliary data for the entire population of interest. Of course, not all surveys have unit-level auxiliary data for the entire population of interest; but when they do, we argue that KBAABB’s artificial populations are realistic, fine-grained, and not biased in favor of any particular SAE model, making KBAABB appropriate for “satisfactory extrapolation” from simulation studies to SAE

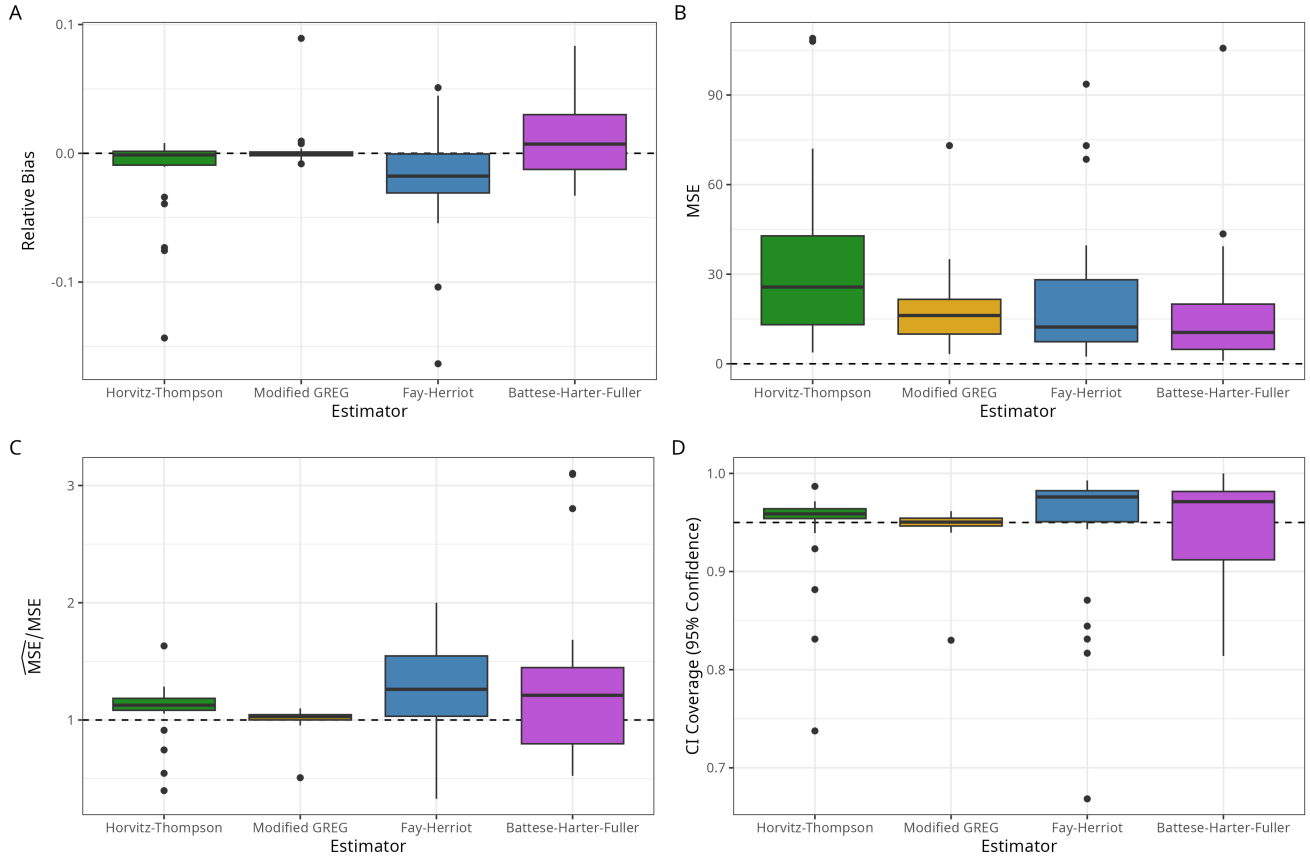


Figure 2: Performance metrics of each estimator for each subsection displayed as side-by-side boxplots. Green represents the Horvitz-Thompson, yellow the modified GREG, blue the area-level EBLUP estimator based on the Fay-Herriot, and purple the unit-level EBLUP estimator based on the Battese-Harter-Fuller. Subfigure A displays the relative bias metric, subfigure B displays the empirical MSE, subfigure C displays the ratio of estimated and empirical MSE, and subfigure D displays the 95% confidence interval coverage rate. For subfigures A-D, the horizontal dashed line has an intercept of 0, 0, 1, and 0.95, respectively, representing the ideal value for each metric.

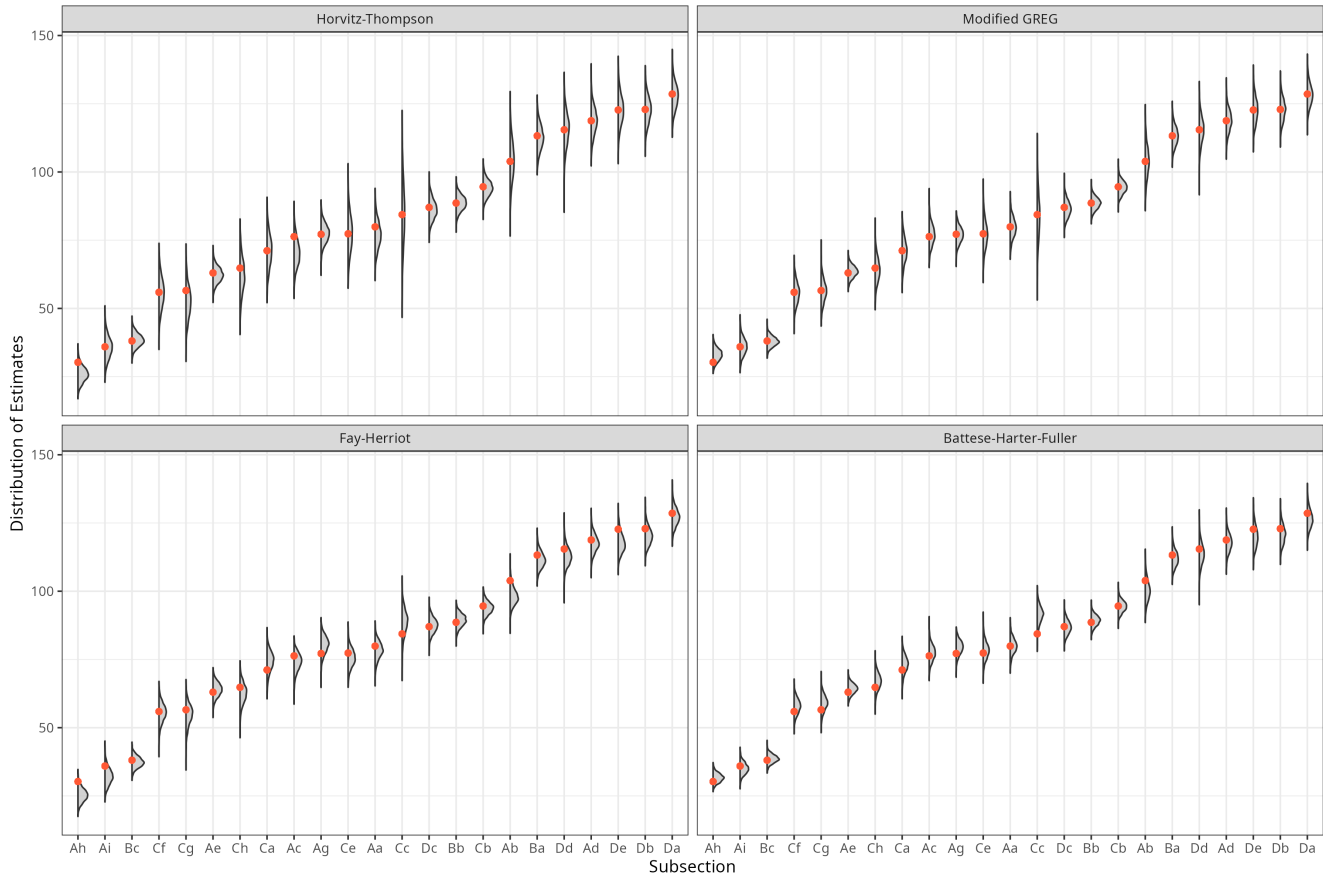


Figure 3: Distributions of estimates produced for each estimator and subsection, along with true KBAABB population parameter value (red dot). The subsections are mapped to the x-axis, and the distribution estimates and true parameter values are mapped to the y-axis. Each panel corresponds to a different estimator. Subsections are ordered by true average basal area from the KBAABB population, least to greatest.

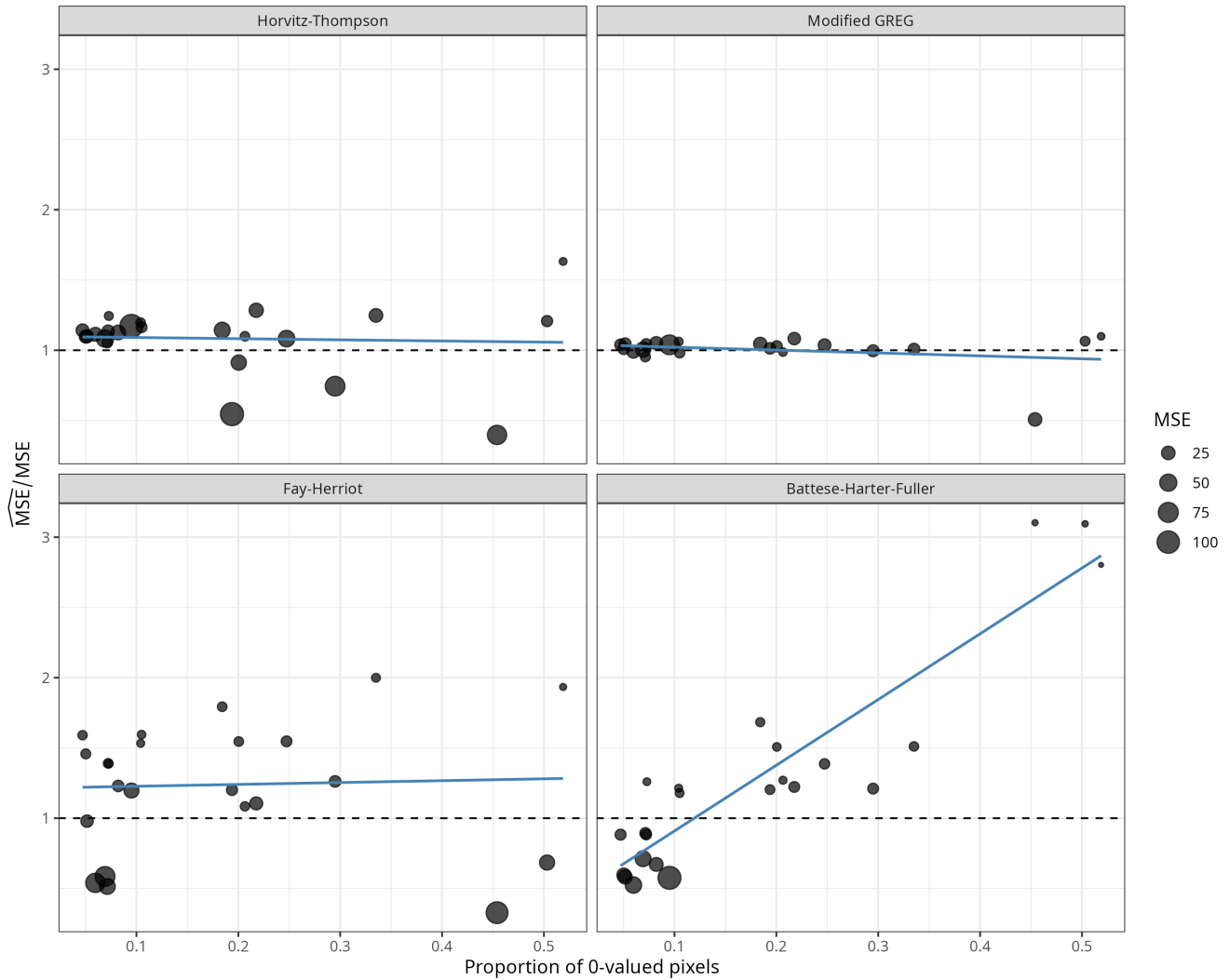


Figure 4: Ratio of estimated MSE and empirical MSE across every domain and estimator by proportion of zero-valued pixels for the response variable in the population, sized by empirical MSE. The MSE ratio is mapped to the y-axis, and the proportion of zero-valued pixels is mapped to the x-axis. Empirical MSE is mapped to point size. The dashed horizontal line has a slope of 0 and intercept of 1, and represents perfect MSE estimation. Blue lines are least-squares regression lines.

estimator performance for the case at hand.

One direction for future work is nonresponse. FIA surveys do experience some nonresponse (for instance, land owners may not admit a survey field crew, or weather conditions may make it impossible to visit a survey plot on schedule), though less than a typical demographic survey and this nonresponse is usually treated as missing at random (MAR) within a given population (Bechtold and Patterson 2005). So far, in generating and sampling from our artificial populations, we have assumed that nonresponse was missing completely at random (MCAR) and ignorable. However, in demographic applications we typically take extra care to ensure that imputation is used appropriately given the posited nonresponse mechanism, which is often MAR or missing not at random (MNAR) rather than MCAR. Appropriate use of KBAABB for generating artificial populations when the survey data had non-MCAR nonresponse is an open question.

Another future direction is the interplay between variable selection for KBAABB matching vs. for SAE modeling. KBAABB is not biased towards any of the common parametric SAE model forms. However, it remains to be seen whether the choice of variables for KBAABB matching may bias the performance estimates of SAE models, when comparing models whose explanatory variables do vs. do not include the matching variables. For the present paper, we side-step this issue by using subject-matter expertise to choose the KBAABB matching variables, and by only using a subset of those variables in the SAE models in our case studies.

We have also not touched on a few complications specific to the FIA data: subplots and condition classes, data vintage, or spatial smoothing. Briefly, condition classes and subplots are more fine-grained levels of detail about the survey data collected at each plot. Our artificial population has been generated only at the plot level so far, and we may extend our methods to work at these other, smaller levels. Meanwhile, the issue of data vintage refers to accounting for the date at which each variable was measured. The survey data comes from a panel design, in which different plots are sampled in different years; and the surveyed pixels'  $X$  variables may not be from the same year as the corresponding  $Y$ . Although most of the  $X$ s change very slowly if at all from year to year (such as elevation or precipitation), others might be more timely (such as NDVI or EVI which should change as forests grow, become harvested, experience wildfires, etc.).

Both our artificial population and our SAE models might benefit from a closer match between the vintages of  $X$  and of  $Y$ , though prior work by FIA researchers suggests that common SAE models are fairly robust to data vintage in this population. Finally, some of the auxiliary variables typically undergo spatial smoothing before use; so it may be appropriate to apply similar spatial smoothing to the imputed  $Y$  values after running KBAABB.

Aside from such details that are specific to our FIA data sources, we believe that KBAABB is a useful approach that could be widely applied to generate artificial populations and evaluate SAEs for any survey where rich, unit-level auxiliary data is available.

**Software:** We are developing an R package `kbaabb` which provides tools for generating an artificial population via KBAABB. The package is available at <https://github.com/graysonwhite/kbaabb/>. While we cannot share the proprietary FIA data used in this paper, the R package includes a worked example based on public data.

We have also created a draft R Shiny application (Chang et al. 2022) for exploring the case study’s artificial population and several estimators. The app can be accessed at <https://civilstat.shinyapps.io/fia-simpop-app/> and the code is available at <https://github.com/ColbyStatSvyRsch/FIA-simpop-app>. For details and screenshots, see Supplemental data, Appendix C.

**Funding:** The authors disclosed receipt of the following financial support for the research, authorship, and/or publication of this article: This work was supported by the National Council for Air and Stream Improvement [grant number FO-SFG-2673 to J.A.W.].

**Declaration of Conflicting Interests:** The authors declare that there is no conflict of interest.

## References

*Agricultural Act of 2014*. 2014. H.R.2642, 113th Congress (2013-2014). <https://www.congress.gov/113/plaws/publ79/PLAW-113publ79.pdf>.

- Agriculture Improvement Act of 2018*. 2018. H.R.2, 115th Congress (2017-2018). <https://www.agriculture.senate.gov/imo/media/doc/Agriculture%20Improvement%20Act%20of%202018.pdf>.
- Alfons, Andreas, Stefan Kraft, Matthias Templ, and Peter Filzmoser. 2011. “Simulation of close-to-reality population data for household surveys with application to EU-SILC.” *Statistical Methods & Applications* 20 (3): 383–407.
- Andridge, Rebecca, Laura Bechtel, and Katherine Jenny Thompson. 2021. “Finding a flexible hot-deck imputation method for multinomial data.” *Journal of Survey Statistics and Methodology* 9 (4): 789–809.
- Andridge, Rebecca R, and Roderick JA Little. 2010. “A review of hot deck imputation for survey non-response.” *International Statistical Review* 78 (1): 40–64.
- Andridge, Rebecca Roberts, and Katherine Jenny Thompson. 2023. “Adapting Nearest Neighbor for Multiple Imputation: Advantages, Challenges, and Drawbacks.” *Journal of Survey Statistics and Methodology* 11 (1): 213–233.
- Baffetta, Federica, Lorenzo Fattorini, Sara Franceschi, and Piermaria Corona. 2009. “Design-based approach to k-nearest neighbours technique for coupling field and remotely sensed data in forest surveys.” *Remote Sensing of Environment* 113 (3): 463–475.
- Battese, George E, Rachel M Harter, and Wayne A Fuller. 1988. “An error-components model for prediction of county crop areas using survey and satellite data.” *Journal of the American Statistical Association* 83 (401): 28–36.
- Bechtold, William A, and Paul L Patterson, eds. 2005. *The Enhanced Forest Inventory and Analysis Program—National Sampling Design and Estimation Procedures*. Gen. Tech. Report SRS-80. U.S. Department of Agriculture, Forest Service, Southern Research Station.
- Brown, Gary, Ray Chambers, Patrick Heady, and Dick Heasman. 2001. “Evaluation of small area estimation methods—an application to unemployment estimates from the UK LFS.” In *Proceedings of Statistics Canada Symposium*, 2001:1–10. Statistics Canada.



- Burrill, EA, AM DiTommaso, JA Turner, SA Pugh, G Christensen, CJ Perry, and BL Conkling. 2021. “The Forest Inventory and Analysis Database: Database Description and User Guide version 9.0.1 for Phase 2. USDA Forest Service,” <http://www.fia.fs.fed.us/library/database-documentation/>.
- Chang, Winston, Joe Cheng, JJ Allaire, Carson Sievert, Barret Schloerke, Yihui Xie, Jeff Allen, Jonathan McPherson, Alan Dipert, and Barbara Borges. 2022. *shiny: Web Application Framework for R*. R package version 1.7.3. <https://CRAN.R-project.org/package=shiny>.
- Chen, Jiahua, and Jun Shao. 2000. “Nearest neighbor imputation for survey data.” *Journal of Official Statistics* 16 (2): 113.
- Cleland, David T, Jerry A Freeouf, James E Keys, Greg J Nowacki, Constance A Carpenter, and W Henry McNab. 2007. *Ecological subregions: sections and subsections of the conterminous United States, presentation scale [1:3,500,000] [CD-ROM]*. A.M. Sloan, cartographer, Gen. Tech. Report WO-76. Washington, DC: U.S. Department of Agriculture, Forest Service.
- Crookston, Nicholas L, and Andrew O Finley. 2008. “yaImpute: an R package for kNN imputation.” *Journal of Statistical Software* 23:1–16. <https://doi.org/10.18637/jss.v023.i10>.
- D’Orazio, Marcello. 2015. “Integration and imputation of survey data in R: the StatMatch package.” *Romanian Statistical Review* 63 (2): 57–68.
- Daly, Christopher, Wayne P Gibson, George H Taylor, Gregory L Johnson, and Phillip Pasteris. 2002. “A knowledge-based approach to the statistical mapping of climate.” *Climate Research* 22 (2): 99–113.
- Dorfman, Alan H. 2018. “Towards a routine external evaluation protocol for small area estimation.” *International Statistical Review* 86 (2): 259–274.
- ECOMAP. 1993. *National hierarchical framework of ecological units*. Unpublished administrative paper. Washington, DC: U.S. Department of Agriculture, Forest Service.

- Fay, Robert E, and Roger A Herriot. 1979. “Estimates of income for small places: an application of James-Stein procedures to census data.” *Journal of the American Statistical Association* 74 (366a): 269–277.
- Finley, Andrew O, Sudipto Banerjee, and David W MacFarlane. 2011. “A hierarchical model for quantifying forest variables over large heterogeneous landscapes with uncertain forest areas.” *Journal of the American Statistical Association* 106 (493): 31–48.
- Frescino, Tracey, and Grayson White. 2022. *FIESTAAnalysis: Analysis Functions for the FIESTA Package*. R package version 0.2.1.
- Frescino, TS, GG Moisen, PL Patterson, C Toney, and GW White. 2023. “FIESTA: A Forest Inventory Estimation and Analysis R Package.” *Ecography Software Note*, <https://doi.org/10.1111/ecog.06428>.
- Heath, Linda S, Mark Hansen, James E Smith, Patrick D Miles, and Brad W Smith. 2009. “Investigation into calculating tree biomass and carbon in the FIADB using a biomass expansion factor approach.” In *Proceedings of the Forest Inventory and Analysis (FIA) Symposium 2008*, 21–23.
- Horvitz, D. G., and D. J. Thompson. 1952. “A generalization of sampling without replacement from a finite universe.” *Journal of the American Statistical Association* 47:663–685.
- Isaki, Cary T, and Wayne A Fuller. 1982. “Survey design under the regression superpopulation model.” *Journal of the American Statistical Association* 77 (377): 89–96.
- James, Gareth, Daniela Witten, Trevor Hastie, and Robert Tibshirani. 2021. *An Introduction to Statistical Learning with Applications in R*. 2nd ed. Springer.
- Lehtonen, Risto, and Ari Veijanen. 2009. “Design-based methods of estimation for domains and small areas.” Chap. 31 in *Handbook of Statistics*, vol. 29B, 219–249. Elsevier.
- Li, Shengqiao. 2019. *FNN: Fast Nearest Neighbor Search Algorithms and Applications*. R package version 1.1.3.1. <https://CRAN.R-project.org/package=FNN>.

- McRoberts, Ronald E, William A Bechtold, Paul L Patterson, Charles T Scott, and Gregory A Reams. 2005. "The enhanced Forest Inventory and Analysis program of the USDA Forest Service: Historical perspective and announcement of statistical documentation." *Journal of Forestry* 103 (6): 304–308.
- Moran, Patrick AP. 1950. "Notes on continuous stochastic phenomena." *Biometrika* 37 (1/2): 17–23.
- Morris, Tim P, Ian R White, and Patrick Royston. 2014. "Tuning multiple imputation by predictive mean matching and local residual draws." *BMC Medical Research Methodology* 14 (75): 1–13.
- Nur, U A M, N T Longford, J E Cade, and D C Greenwood. 2005. "Dealing with incomplete data in questionnaires of food and alcohol consumption." *Statistics in Transition* 7 (1): 111–134.
- Picotte, Joshua J, Daryn Dockter, Jordan Long, Brian Tolk, Anne Davidson, and Birgit Peterson. 2019. "LANDFIRE remap prototype mapping effort: Developing a new framework for mapping vegetation classification, change, and structure." *Fire* 2 (2): 35.
- Rao, John N K, and Isabel Molina. 2015. *Small Area Estimation*. 2nd ed. John Wiley & Sons.
- Rollins, Matthew G. 2009. "LANDFIRE: a nationally consistent vegetation, wildland fire, and fuel assessment." *International Journal of Wildland Fire* 18 (3): 235–249.
- Rubin, Donald B. 2004. *Multiple imputation for nonresponse in surveys*. John Wiley & Sons.
- Rubin, Donald B, and Nathaniel Schenker. 1986. "Multiple imputation for interval estimation from simple random samples with ignorable nonresponse." *Journal of the American Statistical Association* 81 (394): 366–374.
- Schwager, Patrick, and Christian Berg. 2021. "Remote sensing variables improve species distribution models for alpine plant species." *Basic and Applied Ecology* 54:1–13.

- Templ, Matthias, Bernhard Meindl, Alexander Kowarik, and Olivier Dupriez. 2017. “Simulation of synthetic complex data: The R package simPop.” *Journal of Statistical Software* 79 (10): 1–38.
- Tzavidis, Nikos, Li-Chun Zhang, Angela Luna, Timo Schmid, and Natalia Rojas-Perilla. 2018. “From start to finish: a framework for the production of small area official statistics.” *Journal of the Royal Statistical Society, Series A (Statistics in Society)* 181 (4): 927–979.
- U.S. Geological Survey. 2019. *LANDFIRE Elevation*. USGS EROS, Sioux Falls, South Dakota.
- White, Grayson W., Josh K. Yamamoto, Dinan H. Elsyad, Julian F. Schmitt, Niels H. Korsgaard, Jie Kate Hu, George C. Gaines III, Tracey S. Frescino, and Kelly S. McConville. 2024. *Small area estimation of forest biomass via a two-stage model for continuous zero-inflated data*. arXiv: 2402.03263 [stat.AP].
- Wieczorek, Jerzy, and Carolina Franco. 2013. “An Empirical Artificial Population and Sampling Design for Small-Area Model Evaluation.” In *Proceedings of the 2013 Joint Statistical Meetings, American Statistical Association, Alexandria, VA*.
- Wieczorek, Jerzy, Ciara Nugent, and Sam Hawala. 2012. “A Bayesian zero-one inflated beta model for small area shrinkage estimation.” In *Proceedings of the 2012 Joint Statistical Meetings, American Statistical Association, Alexandria, VA*.
- Wojcik, Olek C, Samuel D Olson, Paul-Hieu V Nguyen, Kelly S McConville, Gretchen G Moisen, and Tracey S Frescino. 2022. “GREGORY: A Modified Generalized Regression Estimator Approach to Estimating Forest Attributes in the Interior Western US.” *Frontiers in Forests and Global Change* 4.
- Woodruff, Ralph S. 1966. “Use of a regression technique to produce area breakdowns of the monthly national estimates of retail trade.” *Journal of the American Statistical Association* 61 (314): 496–504.

- Yang, Limin, Suming Jin, Patrick Danielson, Collin Homer, Leila Gass, Stacie M Bender, Adam Case, et al. 2018. “A new generation of the United States National Land Cover Database: Requirements, research priorities, design, and implementation strategies.” *ISPRS Journal of Photogrammetry and Remote Sensing* 146:108–123.
- Yang, Shu, and Jae Kwang Kim. 2019. “Nearest neighbor imputation for general parameter estimation in survey sampling.” In *The Econometrics of Complex Survey Data*, 39:209–234. Emerald Publishing Limited.
- Zanaga, Daniele, Ruben Van De Kerchove, W De Keersmaecker, N Souverijns, Carsten Brockmann, R Quast, Jan Wevers, et al. 2021. “ESA WorldCover 10 m 2020 v100.”

# Appendix to “Assessing small area estimates via bootstrap-weighted k-Nearest-Neighbor artificial populations”

## A Sensitivity to $k$ and Weighted Sampling in our FIA Setting

Besides KBAABB, we also tried generating artificial populations by sampling uniformly from kNN with values of  $k \in \{1, 5, 10, 20, 50, 100\}$ . We expected that  $k$  of 10 or less might be reasonable, while much larger values would lead to artificial populations whose Y values were too close to being uniformly random, but we included larger  $k$  values in order to check this. Indeed, results for KBAABB,  $k=1$ , and  $k=5$  looked fairly similar, but  $k=10$  or above were clearly less realistic. Among KBAABB,  $k=1$ , and  $k=5$ , our forestry subject-matter-experts believed that KBAABB looks more realistic than  $k=1$  or  $k=5$ , and our statisticians believed that KBAABB was better justified than  $k=1$ .

First we checked how  $k$  affected the variability in imputed Y-values within each domain. Using BA (basal area) as an example, Figure 5 shows that for KBAABB as well as kNN with small values of  $k$ , each artificial population’s domain-level SDs are strongly but not perfectly correlated with their original-sample counterparts. As  $k$  grows, we see the correlations get weaker, because for large  $k$  we are drawing uniformly from a large donor pool where the donors do not necessarily resemble the recipient. Indeed, for large enough  $k$  (larger than any shown here), we would simply be sampling donors uniformly from the whole sample and the scatterplot would be essentially horizontal.

Next, we checked the spatial smoothness of the imputed Y-variables, comparing kNN with various  $k$  to the maps for KBAABB (Figure 11) and for X-variables (such as Figures 12 and 13). Spatial smoothness is not our primary goal because we are not yet attempting to fit spatial SAE models, though we may want to fit them in the future. However, we do want to have

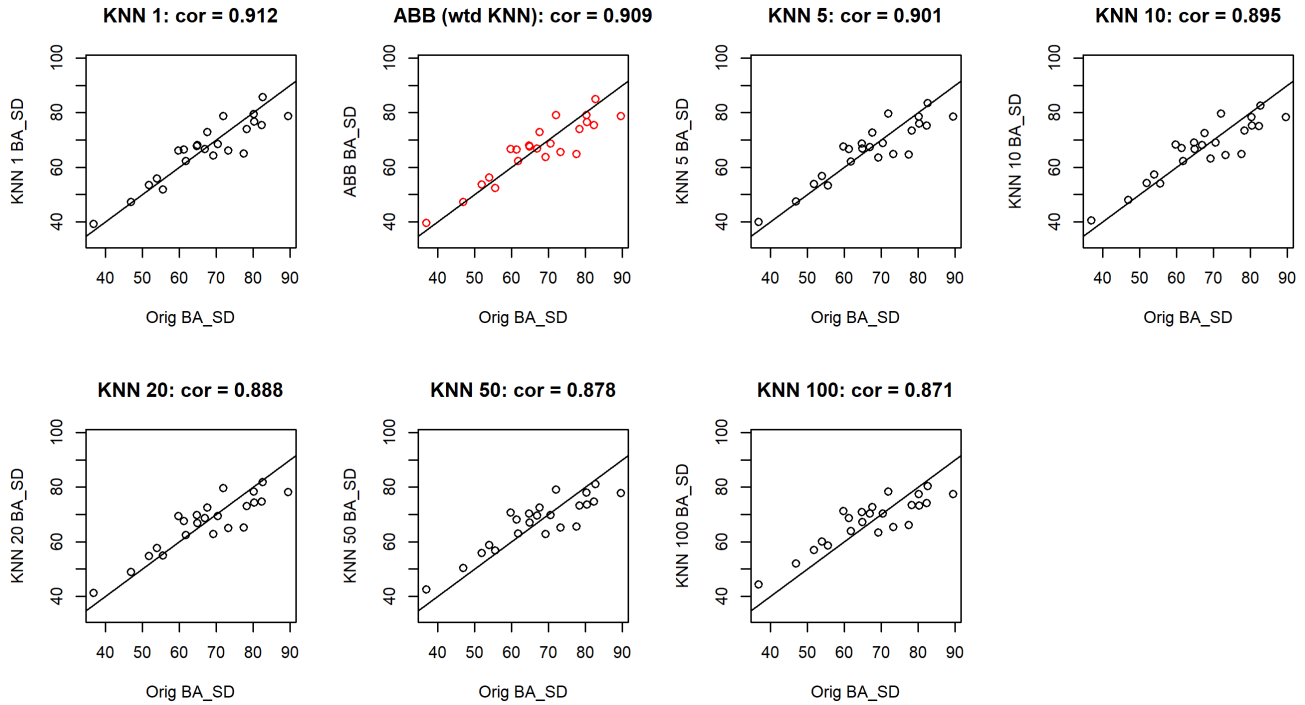
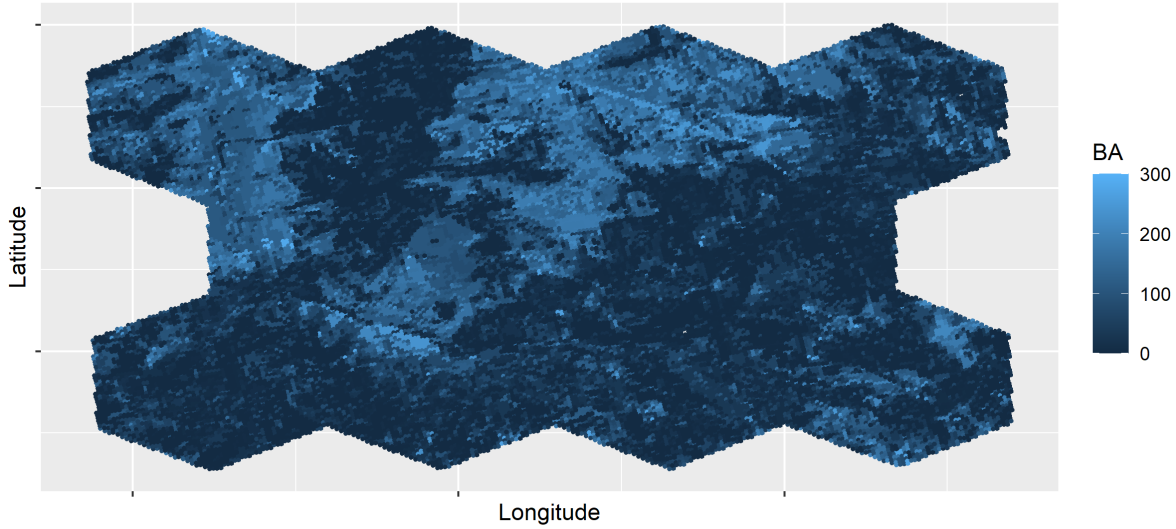


Figure 5: Original vs imputed SDs of BA (basal area) for each subsection, for KBAABB (red) and for kNN at several different  $k$ . All plots show  $y = x$  line as a common reference.

a realistic association between Ys and Xs at the unit level, and if the Xs are spatially smooth but the Ys were clearly not, that would indicate that we probably did not have a realistic association between Ys and Xs in our artificial population. The upper subfigure of Figure 6 shows kNN with  $k=1$ , which looks smoother than Figure 11 did, in the sense that there are many sizeable spatial regions of near-constant Y-values. However, for  $k=5$  (lower subfigure of Figure 6) or greater (Figures 7 and 8), there is substantially more noise, in the sense that many pixels are quite likely to have individual spatial neighbors whose Y value is very far from their own. Although larger-scale spatial patterns can still be discerned in the plots for larger  $k$ , we deemed their lack of small-scale spatial smoothness to indicate unrealistic imputations.

BA (basal area) imputed using kNN with  $k=1$   
in a small portion of subsection M333Ch



BA (basal area) imputed using kNN with  $k=5$   
in a small portion of subsection M333Ch

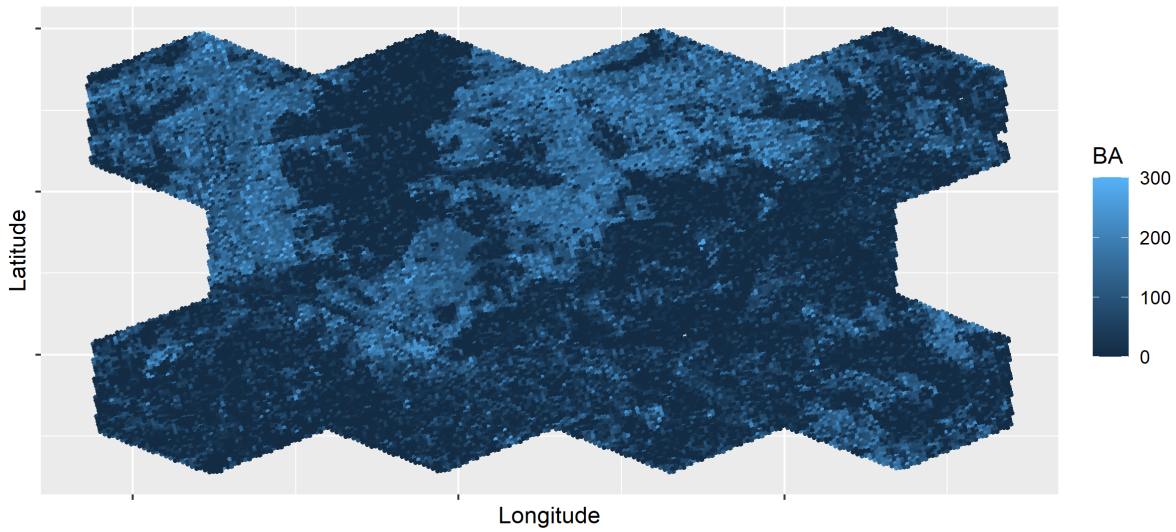
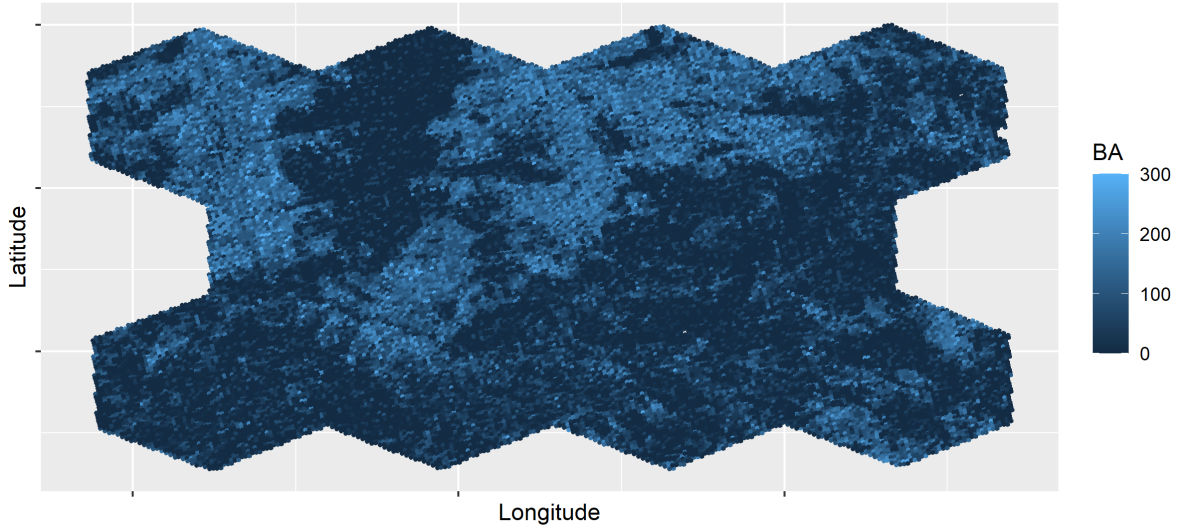


Figure 6: kNN with  $k=1$  (above) and  $k=5$  (below) imputations of BA (basal area) in a portion of subsection M333Ch.



BA (basal area) imputed using kNN with  $k=10$   
in a small portion of subsection M333Ch



BA (basal area) imputed using kNN with  $k=20$   
in a small portion of subsection M333Ch

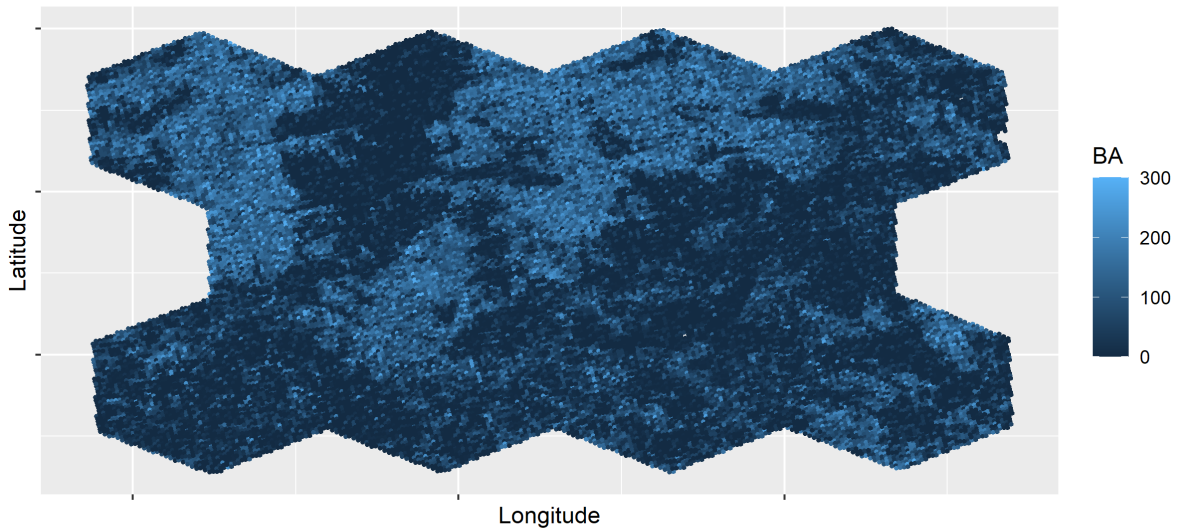
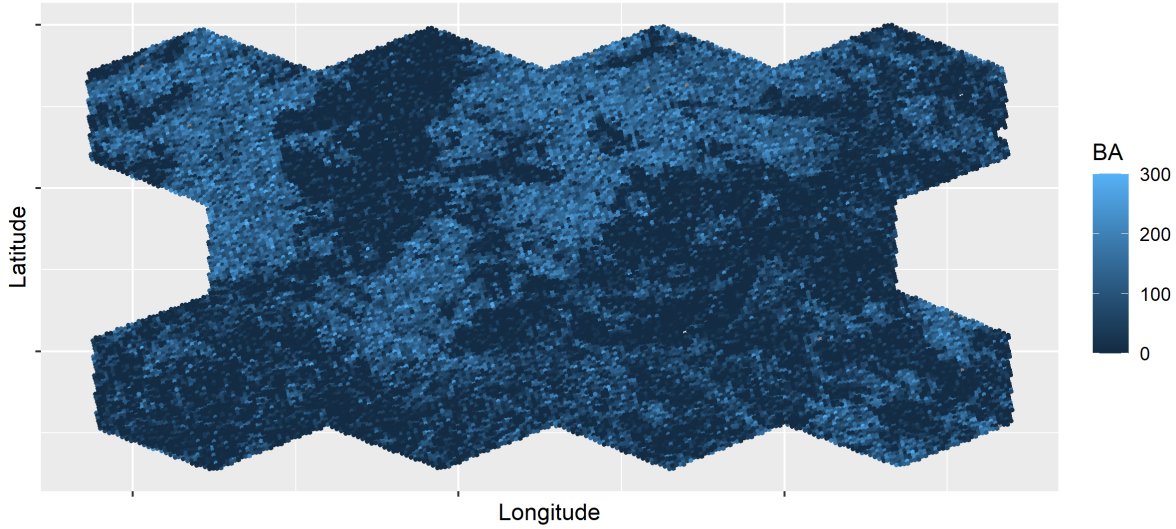


Figure 7: kNN with  $k=10$  (above) and  $k=20$  (below) imputations of BA (basal area) in a portion of subsection M333Ch.

BA (basal area) imputed using kNN with  $k=50$   
in a small portion of subsection M333Ch



BA (basal area) imputed using kNN with  $k=100$   
in a small portion of subsection M333Ch

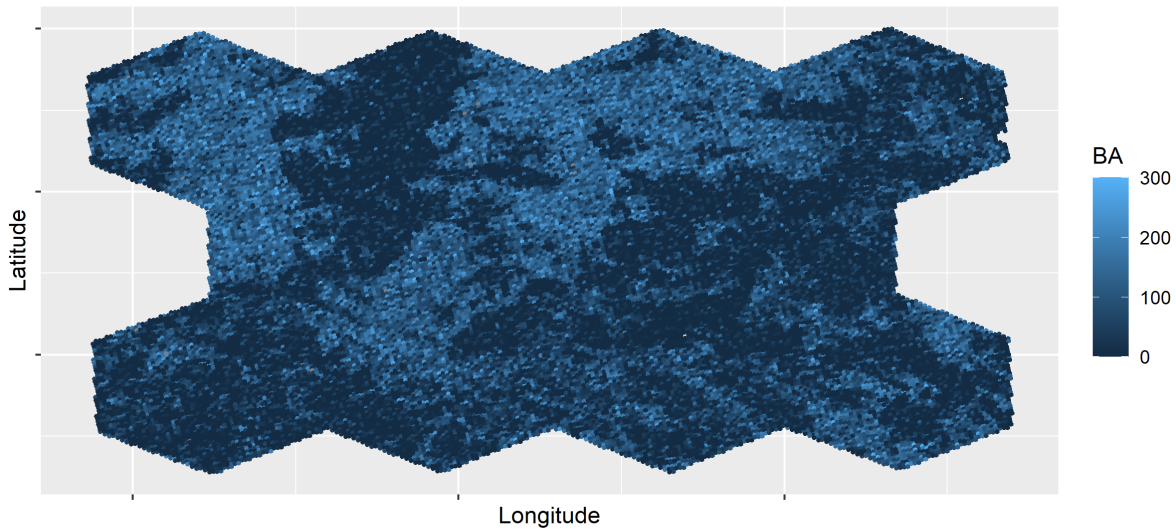


Figure 8: kNN with  $k=50$  (above) and  $k=100$  (below) imputations of BA (basal area) in a portion of subsection M333Ch.

## B KBAABB Implementation and Diagnostics in our FIA Setting

### B.1 KBAABB Implementation in our FIA Setting

As in Algorithm 1, we decided to form strata or “donation classes” using the categorical variable `wc2c1` or World Cover 2-level classification: a “tree or nontree” classification for each pixel, based on satellite measurements. By imputing separately within `wc2c1` classes, we reduce the risk of unrealistically imputing a heavily-forested pixel’s  $Y$  values to an unforested pixel and vice versa.

Next, to avoid the curse of dimensionality, we relied on subject-matter expertise to choose a subset of the quantitative auxiliary variables available for matching. Eight variables were chosen so that they all measured distinct concepts and were thought to be at least somewhat predictive of the  $Y$  variables to be imputed. As a quality check, we confirmed that the selected subset of  $X$  variables had low pairwise correlations within each `wc2c1` donation class, in the full population as well as in the survey sample. At this point, the curse of dimensionality and high variability were deemed not to be major concerns.

Next, we transformed the most heavily skewed of the selected variables to be more symmetric. Right-skewed variables were transformed as  $\log(c_j + X_j)$  and left-skewed variables as  $\log(c_j - X_j)$ , with a separate constant  $c_j$  chosen for each variable  $X_j$  to ensure positive values inside the logarithm.

After this step, we also centered and scaled each of the selected variables to have mean 0 and standard deviation 1 (within each `wc2c1` class separately) on the full-population auxiliary dataset. The same centering and scaling constants (by class and variable) were then applied to the smaller survey sample dataset. This removed the effect of different variables having different units and scales, ensuring that each variable would have effectively the same weight in the kNN matching process (James et al. 2021).

With these selected and transformed variables, we confirmed again that the pairwise correlations were still very small. This allowed us to use simple Euclidean distance, instead of e.g. Ma-

halanobis distance that would account for covariances between variables (Crookston and Finley 2008).

The software we used to carry out the kNN matching step was the `FNN` R package (Li 2019). For every recipient row, we match on the selected, transformed variables to find its donor pool of 10 NNs. We use the bootstrap-probability-based weights described above ( $0.368^{j-1} \times 0.632$ ) to sample one of each recipient’s 10 possible donors. Finally, we impute all 6 of the response  $Y$  variables from that donor to the recipient. If instead we were to impute each response variable independently, our artificial population would not accurately reflect the associations among these variables (Andridge and Little 2010; Nur et al. 2005).

Finally, to define the population means for each  $Y$  variable and domain that are our targets of estimation in the simulation study, we simply take the mean of that  $Y$  variable across all of that domain’s pixels in the artificial population.

See Supplemental data, Appendix B.2, for a description of the diagnostics and sensitivity checks we carried out on the resulting artificial population.

## **B.2 Empirical Diagnostics for KBAABB in our FIA Setting**

To check whether the artificial population generated with KBAABB looked reasonable, we compared the statistical distributions of the imputed  $Y$  variables to the original survey, and we compared the spatial smoothness of the imputed  $Y$  variables to that of similar  $X$  variables. We also looked for imbalances in how often each donor was used, and in how often each recipient’s domain matched the donor’s domain. We repeated these checks for each of the 6  $Y$ -variables and found similar results, so for brevity most examples in this section are illustrated using a single  $Y$  variable: BA (basal area).

First, we confirmed that marginal distributions and pairwise scatterplots from the artificial population resembled the real survey data. For marginal distributions, we compared the original and imputed values of each variable using histograms or eCDFs (empirical cumulative distribution functions), as in Figure 9. Histograms are more familiar to many readers, but eCDFs do not require us to choose a bin size and can also make it easier to compare behavior in the tails.

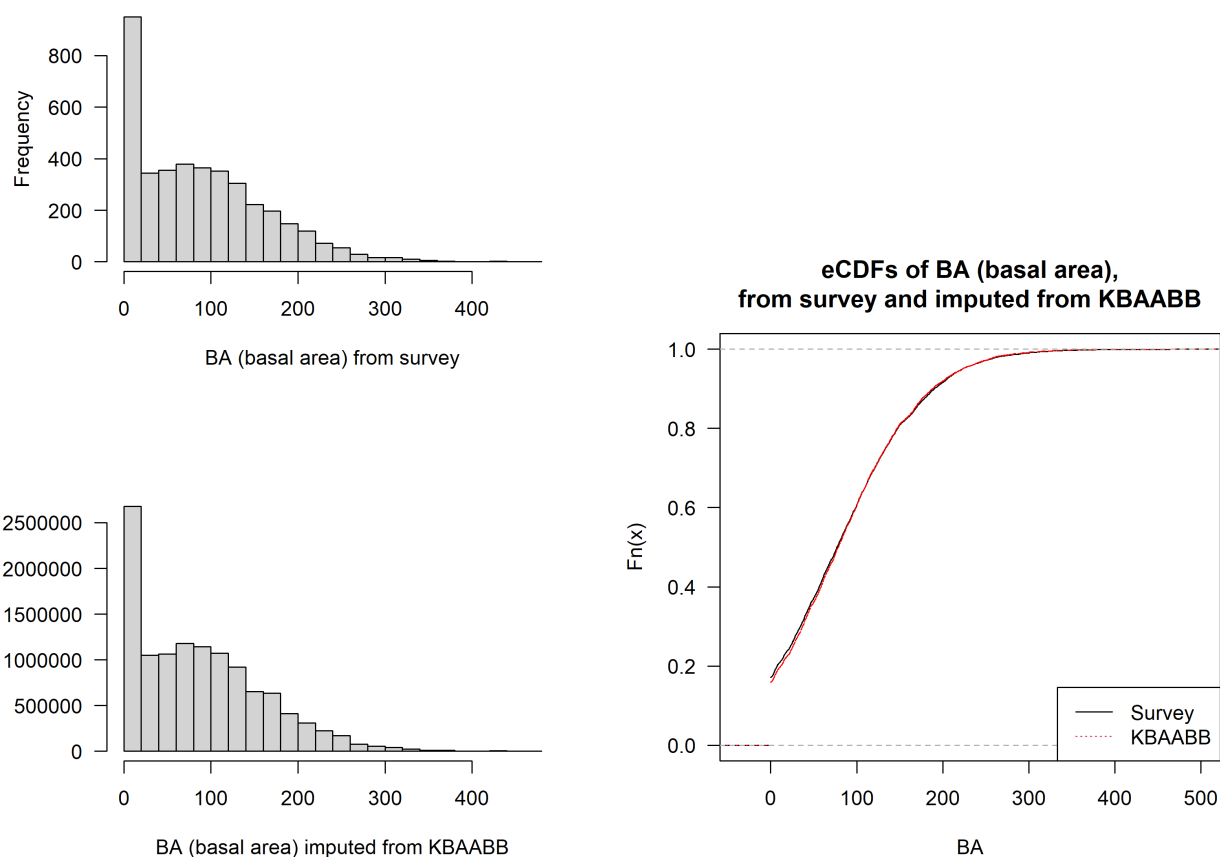


Figure 9: Histograms (left) and empirical CDFs (right) of original vs imputed BA (basal area).

With either graph type, we found that each Y variable’s marginal distribution did not change substantially between the survey and the artificial population. Similarly, we found that pairwise scatterplots (not shown) of the Y variables did not differ noticeably between the survey and the artificial population.

Next, we checked how well the imputed domain-level standard deviations (SDs) match the real survey SDs in each domain. Figure 10 shows that for each Y-variable, the KBAABB artificial population’s domain-level SDs are strongly but not perfectly correlated with their original-sample counterparts. This is a good sign, because if they were perfectly correlated we might simply be reproducing the original sample, while if they had low correlations we might be imputing unrealistic donors to each recipient. For a similar example using kNN with varying values of  $k$ , please see Supplemental data, Appendix A.

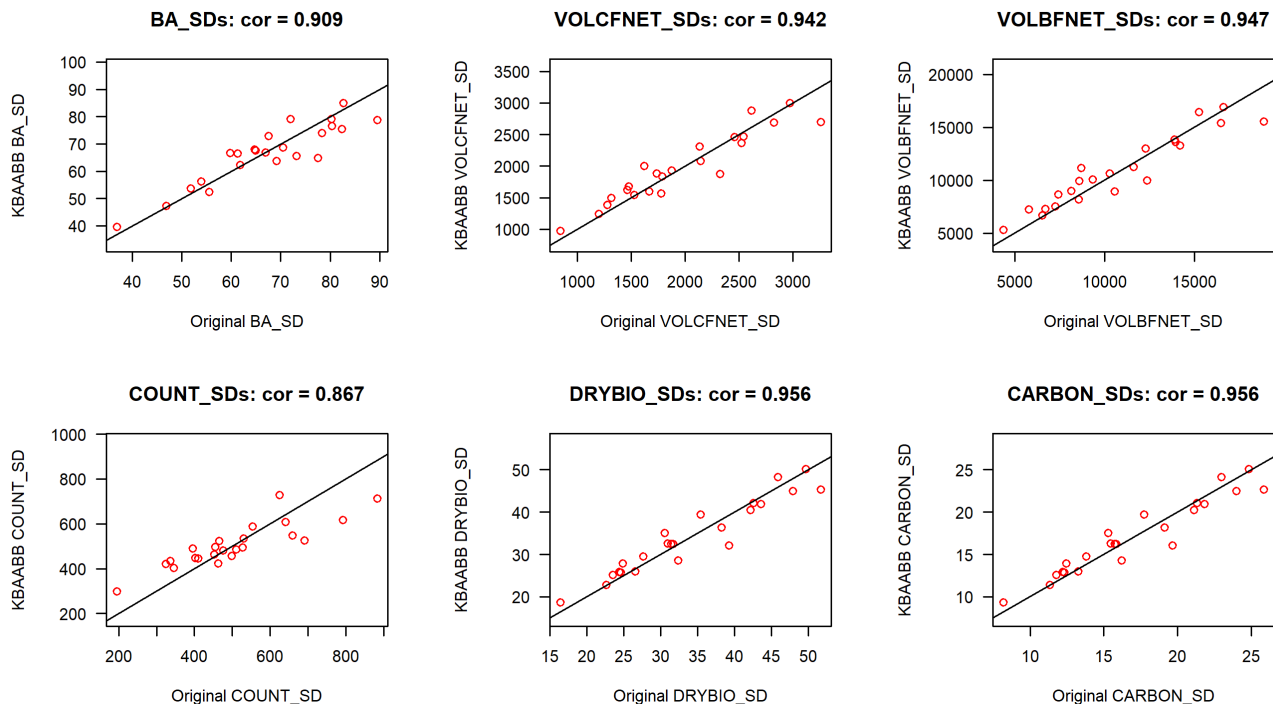


Figure 10: Original vs imputed SDs of each Y-variable for each subsection, using KBAABB. All plots show  $y = x$  line as a common reference.

We also checked whether the spatial smoothness of imputed Ys looks reasonable compared to the spatial smoothness of Xs, for which we have the complete population data. For example, looking at a small portion of the map (zoomed in so that we can see each individual pixel adequately), the spatial patterns in the imputed variable BA (Figure 11) appear to be only a little noisier than spatial patterns for related auxiliary variables `tcc` and `ndvi` (Figures 12 and 13). However, note that many of the auxiliary variables have been spatially smoothed themselves, so it is not surprising that the imputed Ys do not look quite as smooth.

We report further checks in the Supplemental data, Appendix A, where we see similar maps for the other Y variables when using KBAABB, as well as when using kNN with  $k=1$  or 5; but all maps look much too noisy when using kNN with  $k=10$  or greater.

Next, we checked how often each of the 3946 donor rows were used (Figure 14). Recall that for each of the roughly 12 million recipient rows, KBAABB finds its 10 NNs among the donor rows and then uses weighted sampling to choose one donor. Hence, first we checked how often each donor was included in a donor pool of some recipient's 10 NNs (left side of Figure). For

BA (basal area) imputed using KBAABB  
in a small portion of subsection M333Ch

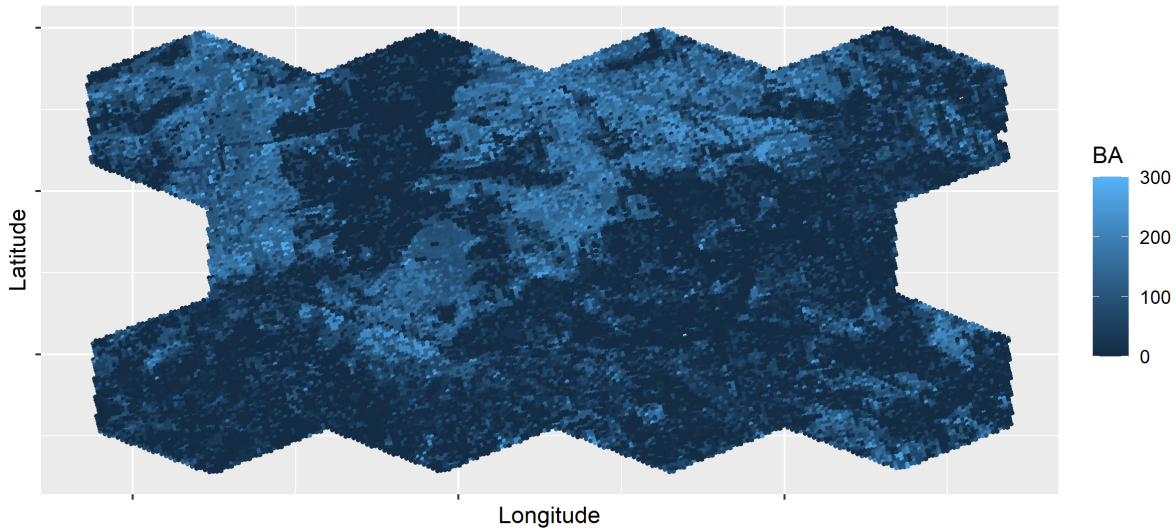


Figure 11: KBAABB imputation of BA (basal area) in a portion of subsection M333Ch.

Auxiliary variable tcc16  
in a small portion of subsection M333Ch

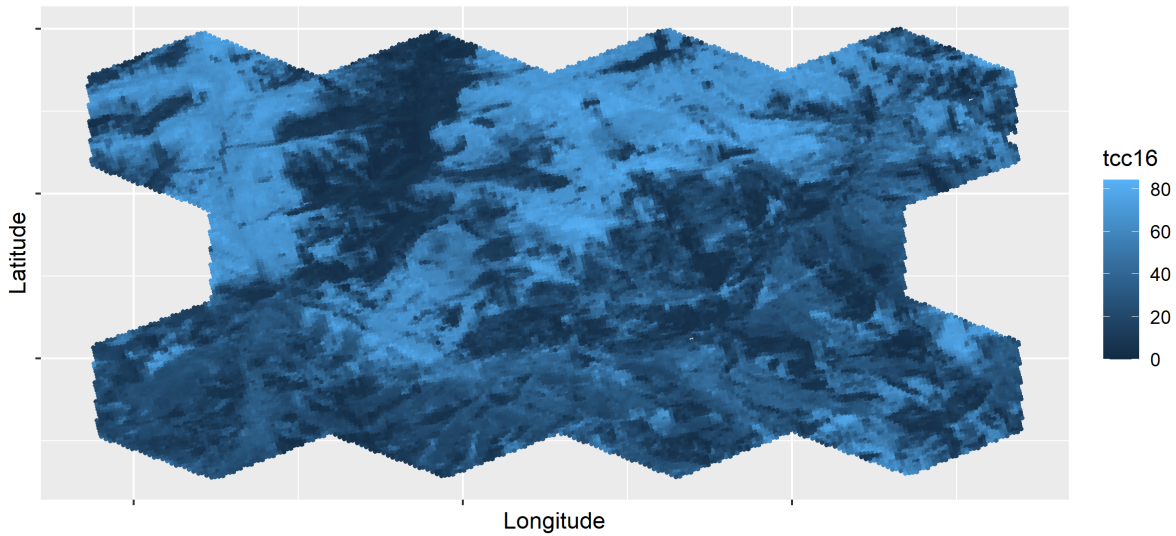


Figure 12: True values of auxiliary variable tcc (tree canopy cover) in a portion of subsection M333Ch.

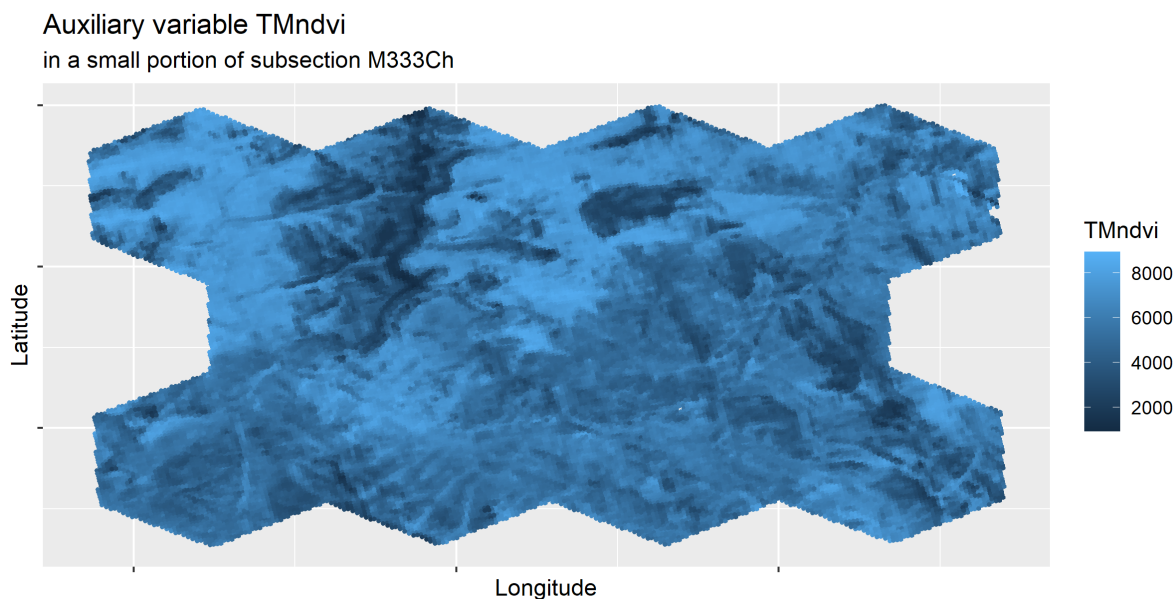


Figure 13: True values of auxiliary variable `ndvi` (Normalized Difference Vegetation Index) in a portion of subsection M333Ch.

both `wc2c1` classes, most donors were chosen to be in 10,000 to 50,000 donor pools, though some were chosen for as many as 69,302 donor pools while others for as few as 1 or 0 donor pools. Every one of the 3101 donors in class 1 (tree) was in a donor pool at least once, and 811 of the 845 donors in class 2 (non-tree) were in a donor pool at least once. Next, we repeated the analysis but to see how often each donor row was actually used as a donor (right side of Figure). For both classes, most donors were actually used for 1,000 to 5,000 recipients, though some were used as many as 9,173 times while others were only used 1 or 0 times. Again every one of the 3101 donors in class 1 was used as a donor at least once, but 790 of the 845 donors in class 2 were used as a donor at least once. In short, only 55 of the possible donors were never used (all in `wc2c1` class 2); 34 of them were never in a donor pool, and the other 11 were in a pool but never happened to be chosen by the weighted sampling. We are not concerned about these few never-used donors, because they all came from the non-tree class, in which most of the Y-variables are all 0s. The other possible donors were typically used a moderate number of times,



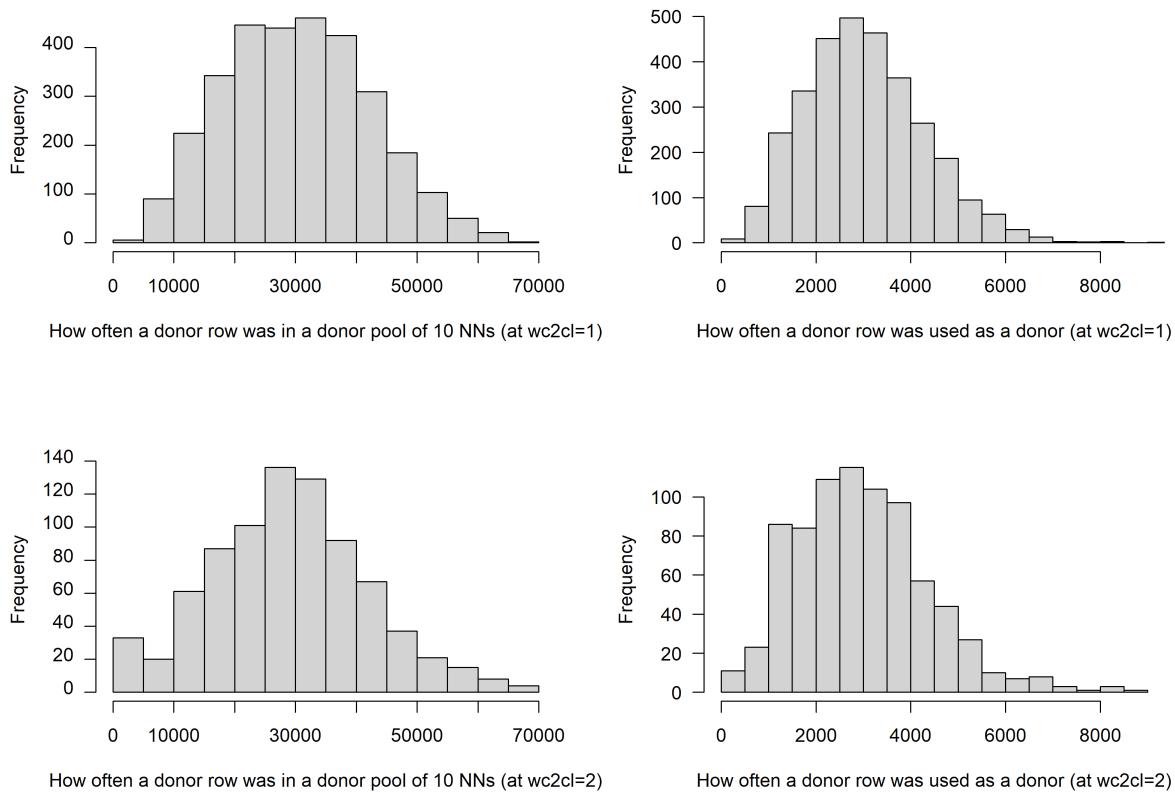


Figure 14: Count of how often each donor row was included in a donor pool of some recipient’s 10 nearest neighbors (left) or actually used as a donor (right), for  $wc2cl$  classes 1 (tree, top) and 2 (non-tree, bottom).

with few over-used or under-used donors.

Finally, recall that our 23 domains are “subsections,” nested within 4 “sections,” ecologically defined so that pixels should tend to be more similar within sections than across them. We cross-tabulated the domain of each donor vs. each recipient to see whether recipients tended to get donors from the same subsection; from a different subsection but still the same section; or from elsewhere (Figure 15). Within each column (recipient), the highest frequencies tend to be in the corresponding row (donor) or another row in the same section (regions separated by black lines), showing that recipients often but not always tended to get donors from the same subsection or at least the same section. If all counts had been only on the main diagonal (each domain’s imputed values all came from the same domain), we would have been concerned that the artificial population is too similar to simply taking copies of the survey sample. On the other

hand, if counts were completely uniform, we would have been concerned that recipients are getting donors which do not actually resemble them. As it is, we feel comfortable seeing that our results fall between these two extremes.

### **B.3 Sampling for Design-Based Simulations in our FIA Setting**

After completing a run of KBAABB, our artificial population consists of around 12 million pixels, corresponding to approximately 4000 hexagons with nearly 3000 pixels per hexagon.

For each replication (“rep”) of a survey sample from this population, we take a sample of one pixel per hexagon, with pixels chosen uniformly at random with each hexagon. This is approximately a form of systematic sampling, since the hexagons uniformly tile the geographic area of interest. Then we drop any locations that happen to fall outside province M333. This lets us carry out design-based simulations which respect the sampling design of the actual survey data. When we fit a given model form to each rep, and then summarize the model’s empirical properties across reps, these properties are reasonable stand-ins for what we could expect to see under repeated sampling from the real sampling design.

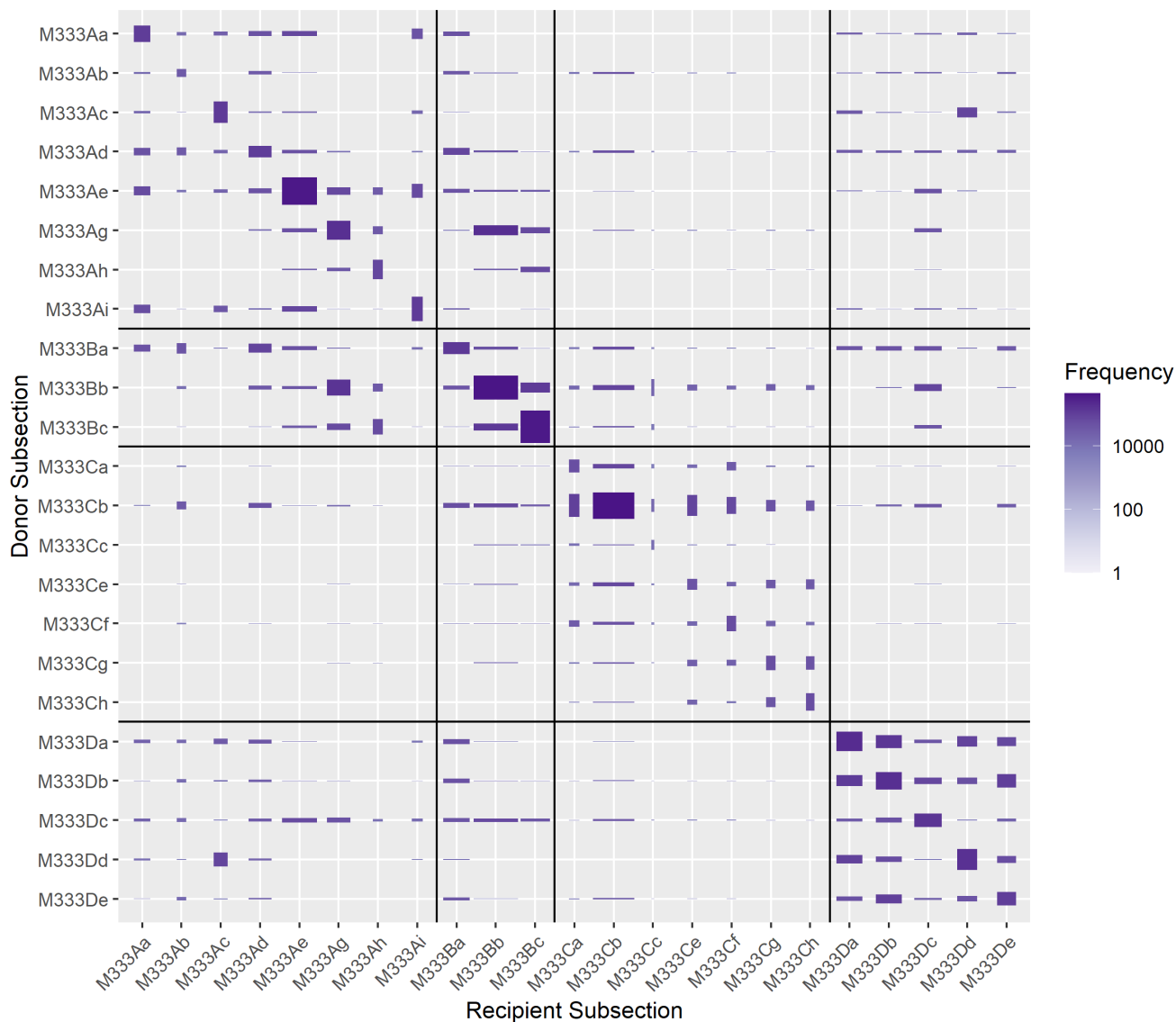


Figure 15: Count of how often donors from each subsection were used by recipients in each subsection. Box widths (fixed within each column) are proportional to the total number of pixels in each recipient subsection. Box heights (varying within each column) are proportional to the number of times a donor from that subsection was used for a recipient in that subsection, scaled so that boxes along the main diagonal would be squares if each conditional proportion (how often did that recipient use donors from its own subsection?) was equal to the overall proportion (31% of recipient pixels got donors from their own subsection).

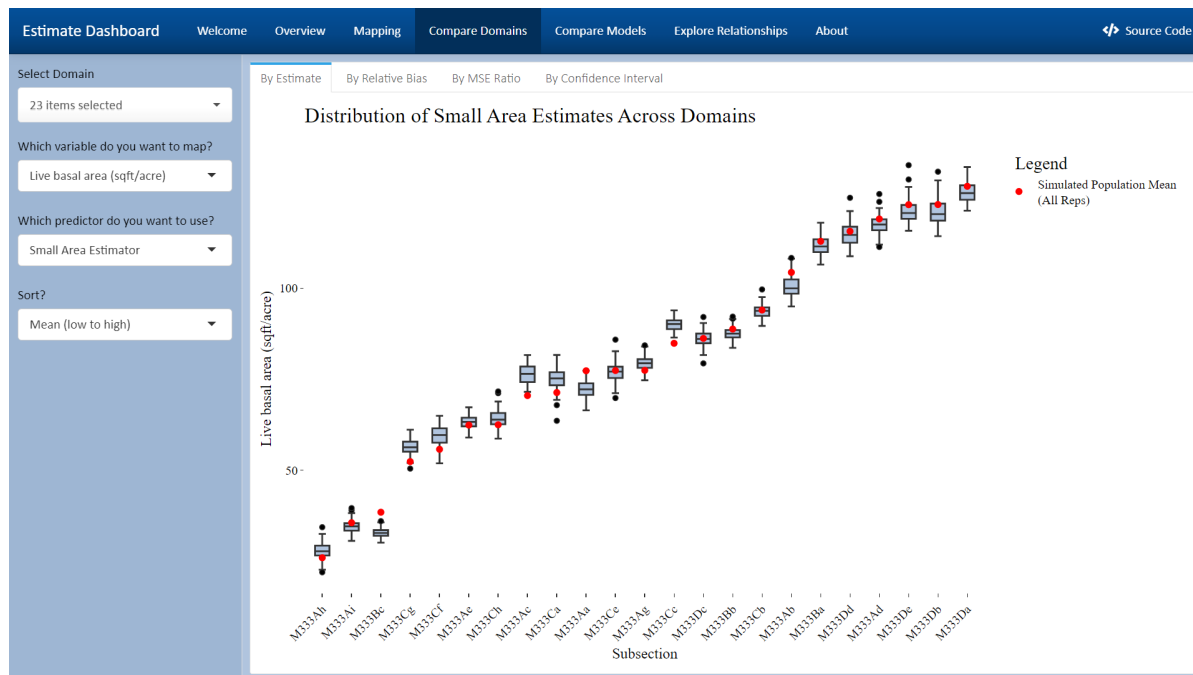


Figure 16: Screenshot of R Shiny app showing SAEs from a model for Basal Area, for each of 23 domains. Each boxplot summarizes 100 reps.

## C Exploring KBAABB Output with an R Shiny App

Alongside this paper we have created a draft R Shiny application (Chang et al. 2022) for exploring the artificial population and a few estimators. The app can be accessed at <https://civilstat.shinyapps.io/fia-simpop-app/> and the code is available at <https://github.com/ColbyStatSvyRsch/FIA-simpop-app>.

For each of the 100 reps currently used in the R Shiny app, on each of the 23 domains we calculate three estimators: a direct Horvitz-Thompson estimator, a post-stratified estimator, and a small area estimator using the unit-level Battese-Harter-Fuller model. Each model is specified on the app’s “About” page. Finally, for every domain and each of these three estimators, we calculate the relative bias; the  $\widehat{\text{MSE}}/\text{MSE}$  ratio; and the 95% CI coverage, as in Section 3.

The app includes a “Compare Domains” page, in which the user can select one or more domains; a response variable; an estimator; and how to sort the domains. For these selections, boxplots for each of the 23 domains are used to show the distribution across 100 reps of estimates (Figure 16, lower subfigure), relative biases (Figure 17), MSE ratios (Figure 18), or CI coverages (Figure 19) on different tabs within the page.

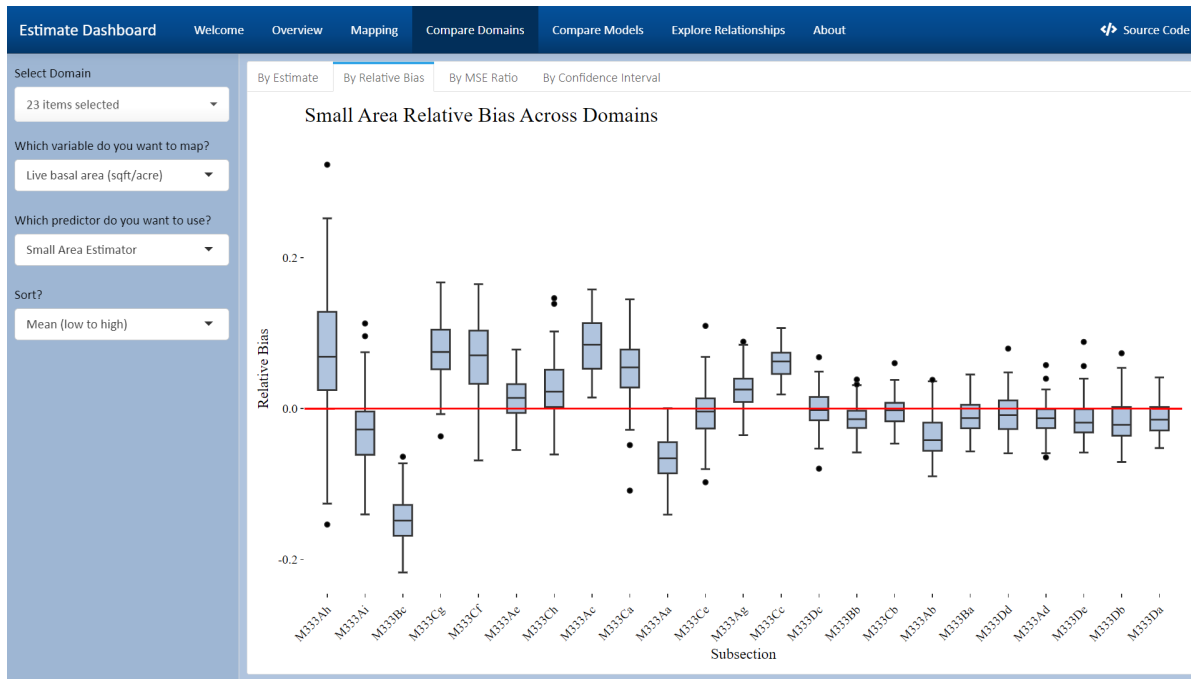


Figure 17: Screenshot of R Shiny app showing the relative biases of SAE models for Basal Area, for each of 23 domains. Each boxplot summarizes 100 reps.

The next page is “Compare Models” (Figure 20), which is similar to “Compare Domains” except that it shows all three estimators for one domain, rather than multiple domains for one estimator.

Finally, the “Explore Relationships” page (Figure 21) allows the user to view scatterplots of any response variable against any auxiliary variable, faceted into small multiples—one for each domain. This can be useful for model diagnostics: are there some auxiliary variables for which the unit-level models should differ substantially across domains?

We have also included a Mapping page (Figure 22), which shows a choropleth map of each domain’s estimates for a given estimator and rep. This allows users to see any spatial patterns that may be present in the estimates, as well as to explore how much these patterns vary across reps.

We are currently using this R Shiny app to help us check and compare small area models ourselves. As we develop better models and concrete advice for users of SAEs for this population, we expect that the R Shiny app will also become useful for disseminating such advice to the diverse group of FIA users.

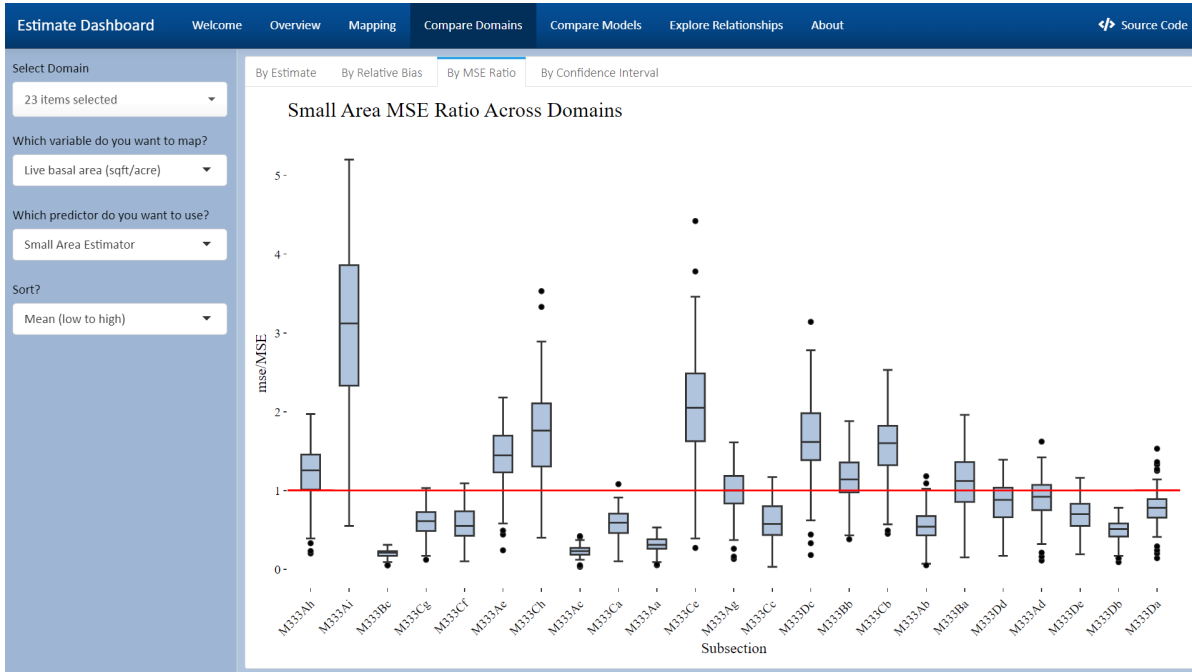


Figure 18: Screenshot of R Shiny app showing the  $\widehat{MSE}/MSE$  ratios of SAE models for Basal Area, for each of 23 domains. Each boxplot summarizes 100 reps.

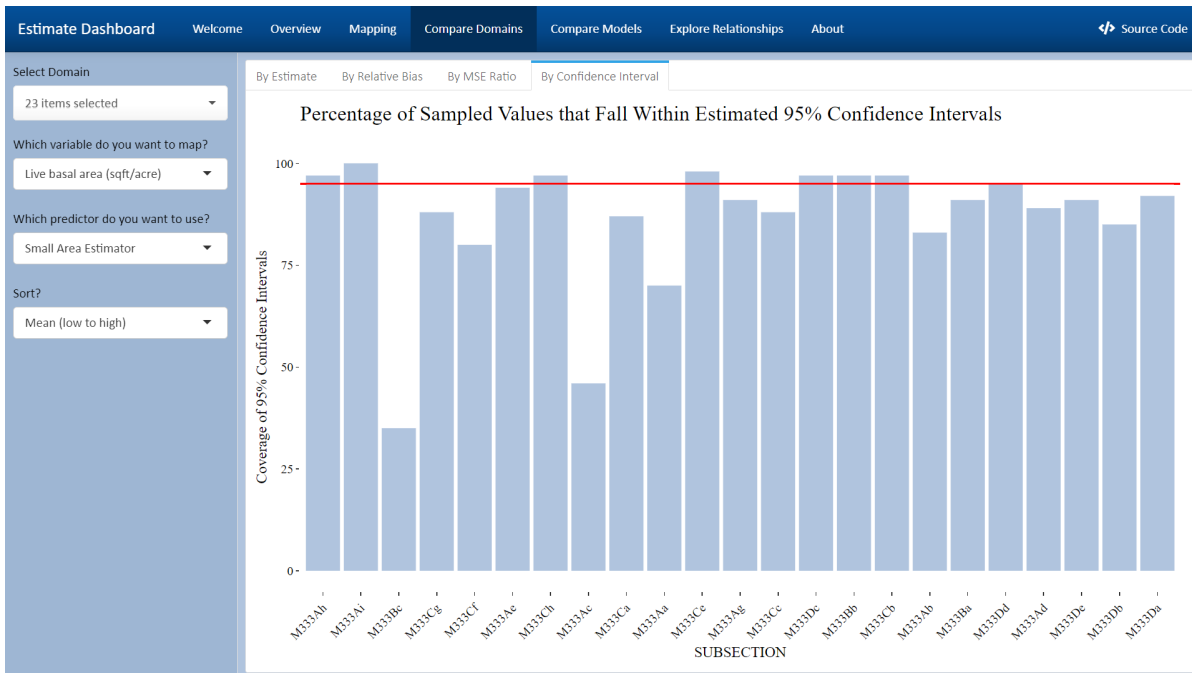


Figure 19: Screenshot of R Shiny app showing coverage of SAE models' 95% confidence intervals for Basal Area, for each of 23 domains. Each bar summarizes 100 reps.

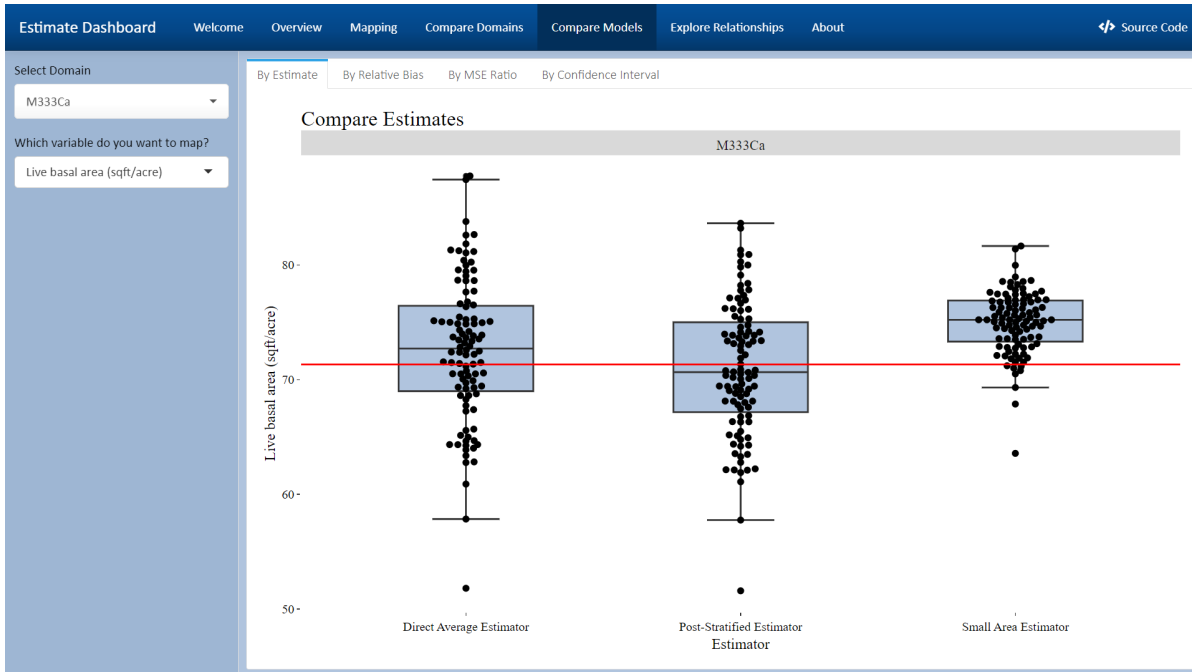


Figure 20: Screenshot of R Shiny app showing the estimates under three estimators for Basal Area, for one selected domain. Each boxplot summarizes 100 reps.

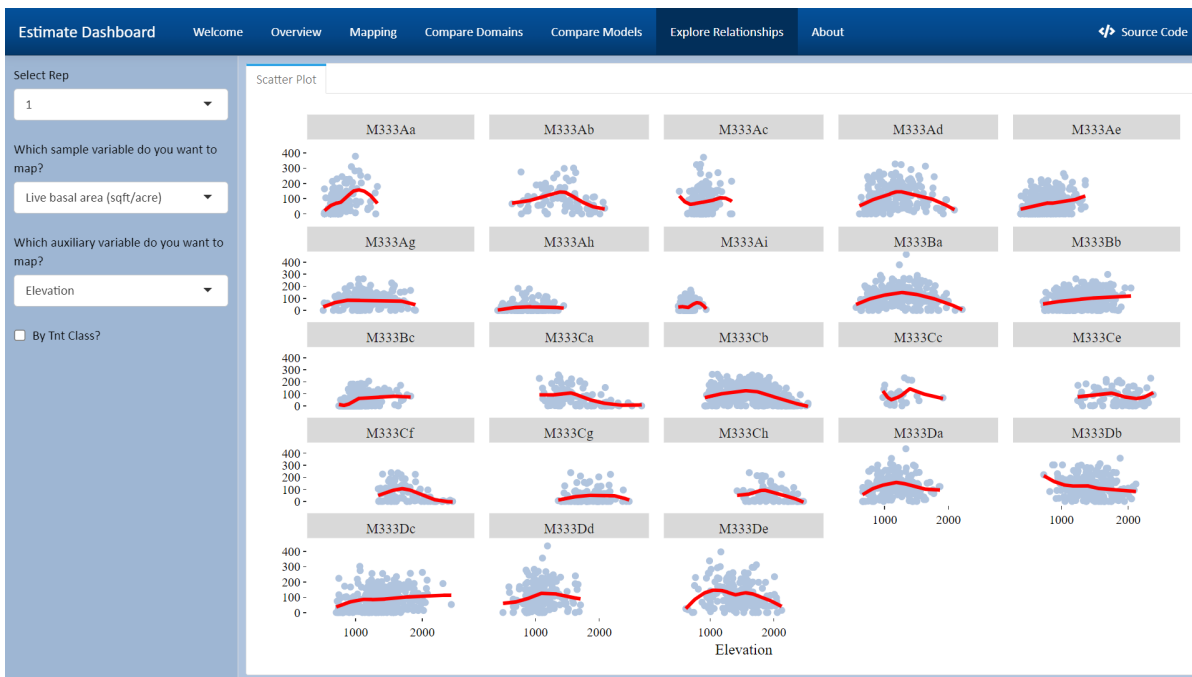


Figure 21: Screenshot of R Shiny app showing scatterplots of Basal Area against Elevation, for each of 23 domains, for sampled pixels in the first rep only.

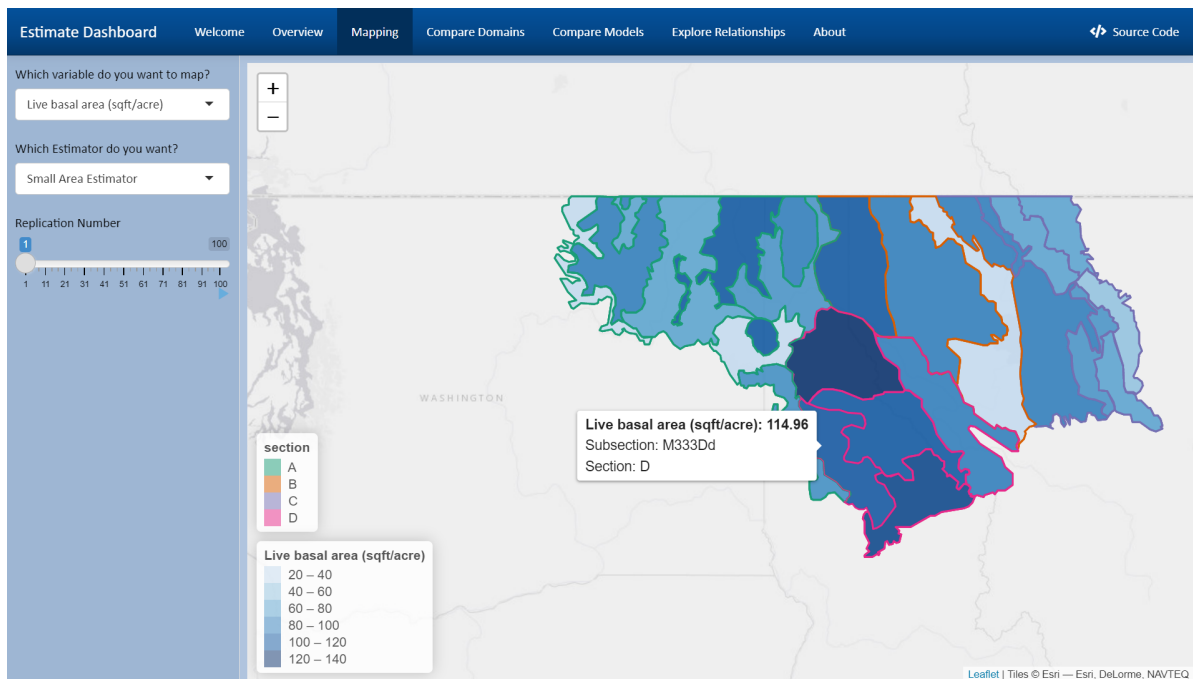


Figure 22: Screenshot of R Shiny app showing a choropleth map of SAE estimates for Basal Area for all of the 23 domains. One rep is selected, but the “Play” button can be used to start an animation to show the map for different reps.